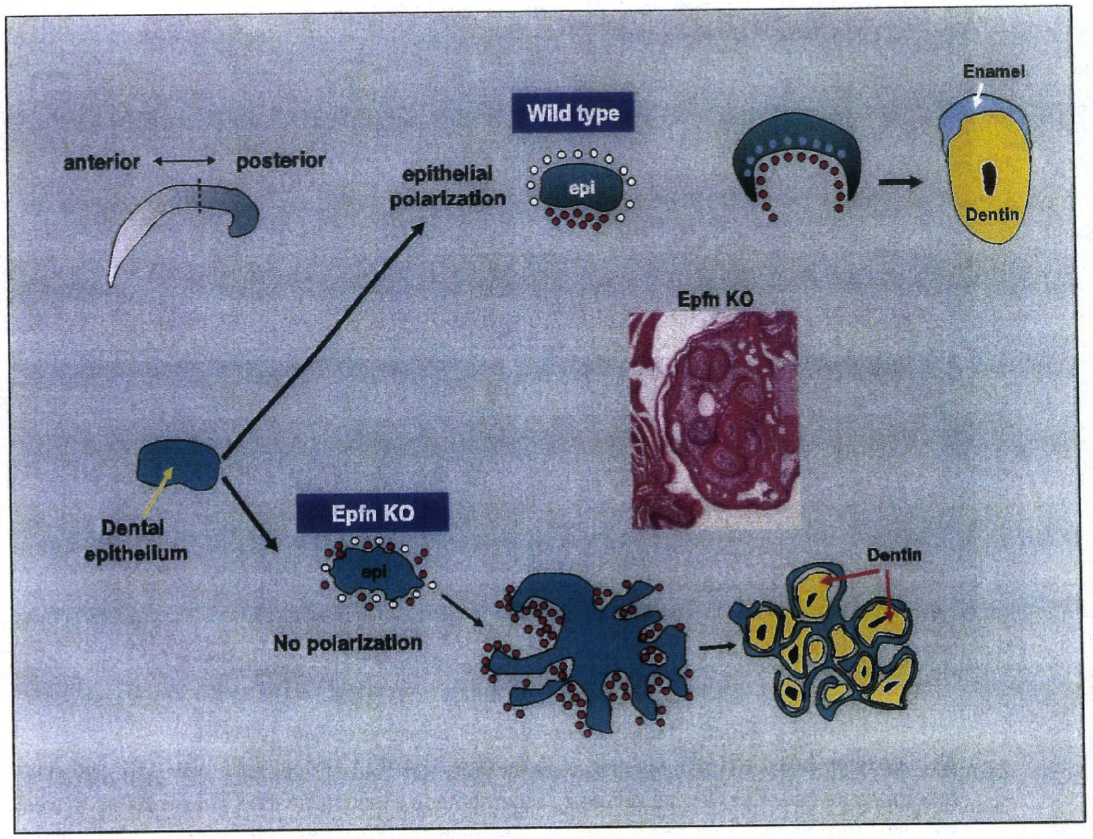

Fig. 3 Proposed model for multiple tooth formation in *Epfn* KO mouse incisors
This scheme shows a frontal section view of mouse incisors. In wild type incisor only the labial side of dental epithelial cells can polarize and differentiate into enamel-forming ameloblasts (blue). The lingual side of dental epithelial cells differentiates into Hertwig's epithelial root sheath and does not differentiate into enamel-forming ameloblasts. The adjacent dental mesenchymal cells (white) interact with dental epithelial cells and differentiate into dentin-forming odontoblasts (red). In KO mice, the dental epithelium is not well polarized and randomly keeps invaginating into dental mesenchyme. A tip of the invagination of dental epithelium starts to interact with adjacent mesenchymal calls and eventually the adjacent mesenchymal cells are induced to differentiate into dentin-forming odontoblasts (Red). The migrating dental epithelial cells in *Epfn* KO mice never differentiate into ameloblasts. As a result, no enamel is formed on the surface of incisors. A cluster of odontoblasts is formed and develops supernumerary teeth, which lack enamel.

Supernumerary Tooth Formation and Defect of Enamel in *Epfn* KO Mice

One of the striking phenotypes of *Epfn* KO mice is supernumerary tooth formation in both incisors and molars. Especially at the incisor region of *Epfn* KO mice, supernumerary incisors were continuously produced with aging. We found nearly 50 incisors in 6-month-old *Epfn* KO mice. Dental epithelial cells deficient of *Epfn* fail to polarize and are completely blocked from differentiating into enamel-forming ameloblasts. As a result, no enamel formation is observed in *Epfn* KO mice (Fig. 2B, 2D). Undifferentiated dental epithelial cells in mutant mice sustain immature states of cell physiology such as those in the bud stage of tooth development. Dental epithelium of mutant mice keeps invaginating into mesen-

chymal tissue randomly and the interactions between dental epithelium and mesenchyme occurr sequentially (Fig. 3). The mesenchymal cells adjacent to undifferentiated dental epithelium are induced to differentiate into dental mesenchymal cells that further differentiating into odontoblasts. The randomly induced odontoblasts in mutant mice start producing dentin matrix and form tooth structures such as dentin and dental pulp. This finding suggests that the dental mesenchyme can be induced by interaction with undifferentiated dental epithelial cells and there is no limitation to dental mesenchymal tissue production. In sum, the dental epithelium regulates the number of teeth, and maintaing the undifferentiated state of dental epithelium is a key for the creation of bioteeth by tissue engineering techniques.

Recently, it has been reported that the continuous activation of Wnt β-catenin signalling in the oral epithelium by cross-mating of $\beta\text{-}cat^{\Delta ex3K14/+}$ and *K14-Cre* ; $Apc^{cko/cko}$ mice induces supernumerary tooth formation[27,28]. Histological analysis has revealed that the dental epithelial branching in molar tooth buds is similar to the observations in *Epfn* KO tooth buds. However there are some differences in supernumerary tooth formation between *Epfn* KO mice and $\beta\text{-}cat^{\Delta ex3K14/+}$ mice. In *Epfn* KO mice, multiple branching of dental epithelium in a tooth bud was observed after the bud stage. Importantly, multiple tooth buds were formed from a single dental lamina in *Epfn* KO mice. On the other hand, in $\beta\text{-}cat^{\Delta ex3K14/+}$ mice, supernumerary teeth were formed not only by branching of dental epithelium but also by multiple placode formations. Because $\beta\text{-}cat^{\Delta ex3K14/+}$ mice were created by cross-mating $K14\text{-}Cre^{Tg/+}$ mice and $\beta\text{-}cat^{\Delta ex3flox/+}$ mice, the entire epithelial tissue including oral ectoderm and dental epithelium was expressing stabilized β-catenin, which mimics the continuous activation of Wnt *β-cat* signalling. Therefore the multiple placode formation in $\beta\text{-}cat^{\Delta ex3K14/+}$ mice should be formed by a similar mechanism to other Wnt signalling arranged mouse models in ectodermal appendages and showld developed via different mechanism from that of *Epfn* KO mice[29—32]. In sum, the dental epithelial branching into dental mesenchyme observed in *Epfn* KO tooth buds could be linked to the activation of Wnt β-catenin signalling. We are analyzing the molecular interaction between Epfn and molecules involved in Wnt β-catenin signalling to elucidate the onset mechanism of supernumerary tooth formation.

Conclusion

The precise balance between cell proliferation and cytodifferentiation is important in tooth development to form a functional shape and size of tooth crown. We demonstrate that Epfn regulates dental epithelial cell proliferation and differentiation. *Epfn* KO mice show impaired tooth morphogenesis and develop supernumerary teeth with a lack of enamel due to a defect in dental epithelial cell differentiation. Thus, Epfn orchestrates tooth development and morphogenesis by controlling cell proliferation and differentiation.

References

1) Nakamura, T., Unda, F., de-Vega, S., Vilaxa, A., Fukumoto, S., Yamada, K. M. and Yamada, Y. : The Kruppel-like factor epiprofin is expressed by epithelium of developing teeth, hair follicles, and limb buds and promotes cell proliferation. J. Biol. Chem. **279** : 626—634, 2004.
2) Suske, G., Bruford, E. and Philipsen, S. : Mammalian SP KLF transcription factors : bring in the family. Genomics **85** : 551—556, 2005.
3) Gidoni, D., Dynan, W. S. and Tjian, R. : Multiple specific contacts between a mammalian transcription factor and its cognate promoters. Nature **312** : 409—413, 1984.
4) Zhao, C. and Meng, A. : Sp1-like transcription factors are regulators of embryonic development in vertebrates. Dev. Growth. Differ. **47** : 201—211, 2005.
5) Black, A. R., Black, J. D. and Azizkhan-Clifford, J. : Sp1 and kruppel-like factor family of transcription factors in cell growth regulation and cancer. J. Cell. Physiol. **188** : 143—160, 2001.
6) Ghayor, C., Chadjichristos, C., Herrouin, J. F., Ala-Kokko, L., Suske, G., Pujol, J. P. and Galera, P. : Sp3 represses the Sp1-mediated transactivation of the human COL2A1 gene in primary and de-differentiated chondrocytes. J. Biol. Chem. **276** : 36881—

36895, 2001.

7) Lomberk, G. and Urrutia, R. : The family feud : turning off Sp1 by Sp1-like KLF proteins. Biochem. J. **392** : 1—11, 2005.

8) Baur, F., Nau, K., Sadic, D., Allweiss, L., Elsasser, H. P., Gillemans, N., de Wit, T., Kruger, I., Vollmer, M., Philipsen, S. and Suske, G. : Specificity protein 2 (Sp2) is essential for mouse development and autonomous proliferation of mouse embryonic fibroblasts. PLoS. One. **5** : e9587, 2010.

9) Marin, M., Karis, A., Visser, P., Grosveld, F. and Philipsen, S. : Transcription factor Sp1 is essential for early embryonic development but dispensable for cell growth and differentiation. Cell **89** : 619—628, 1997.

10) Bouwman, P., Gollner, H., Elsasser, H. P., Eckhoff, G., Karis, A., Grosveld, F., Philipsen, S. and Suske, G. : Transcription factor Sp3 is essential for post-natal survival and late tooth development. EMBO. J. **19** : 655—661, 2000.

11) Van Loo, P. F., Bouwman, P., Ling, K. W., Middendorp, S., Suske, G., Grosveld, F., Dzierzak, E., Philipsen, S. and Hendriks, R. W. : Impaired hematopoiesis in mice lacking the transcription factor Sp3. Blood **102** : 858—866, 2003.

12) Supp, D. M., Witte, D. P., Branford, W. W., Smith, E. P. and Potter, S. S. : Sp4, a member of the Sp1-family of zinc finger transcription factors, is required for normal murine growth, viability, and male fertility. Dev. Biol. **176** : 284—299, 1996.

13) Gollner, H., Bouwman, P., Mangold, M., Karis, A., Braun, H., Rohner, I., Del Rey, A., Besedovsky, H. O., Meinhardt, A., van den Broek, M., Cutforth, T., Grosveld, F., Philipsen, S. and Suske, G. : Complex phenotype of mice homozygous for a null mutation in the Sp4 transcription factor gene. Genes. Cells. **6** : 689—697, 2001.

14) Harrison, S. M., Houzelstein, D., Dunwoodie, S. L. and Beddington, R. S. : Sp5, a new member of the Sp1 family, is dynamically expressed during development and genetically interacts with Brachyury. Dev. Biol. **227** : 358—372, 2000.

15) Nakashima, K., Zhou, X., Kunkel, G., Zhang, Z., Deng, J. M., Behringer, R. R. and de Crombrugghe, B. : The novel zinc finger-containing transcription factor osterix is required for osteoblast differentiation and bone formation. Cell **108** : 17—29, 2002.

16) Bell, S. M., Schreiner, C. M., Waclaw, R. R., Campbell, K., Potter, S. S. and Scott, W. J. : Sp8 is crucial for limb outgrowth and neuropore closure. Proc. Natl. Acad. Sci. USA. **100** : 12195—12200, 2003.

17) Kawakami, Y., Esteban, C. R., Matsui, T., Rodriguez-Leon, J., Kato, S. and Izpisua Belmonte, J. C. : Sp8 and Sp9, two closely related buttonhead-like transcription factors, regulate Fgf8 expression and limb outgrowth in vertebrate embryos. Development. **131** : 4763—4774, 2004.

18) Bouwman, P. and Philipsen, S. : Regulation of the activity of Sp1-related transcription factors. Mol. Cell. Endocrinol. **195** : 27—38, 2002.

19) Thesleff, I., Vaahtokari, A. and Vainio, S. : Molecular changes during determination and differentiation of the dental mesenchymal cell lineage. J. Biol. Buccale. **18** : 179—188, 1990.

20) Warshawsky, H. and Smith, C. E. : Morphological classification of rat incisor ameloblasts. Anat. Rec. **179** : 423—446, 1974.

21) Smith, C. E. : Cellular and chemical events during enamel maturation. Crit. Rev. Oral. Biol. Med. **9** : 128—161, 1998.

22) Sonoda, A., Iwamoto, T., Nakamura, T., Fukumoto, E., Yoshizaki, K., Yamada, A., Arakaki, M., Harada, H., Nonaka, K., Nakamura, S., Yamada, Y. and Fukumoto, S. : Critical role of heparin binding domains of ameloblastin for dental epithelium cell adhesion and ameloblastoma proliferation. J. Biol. Chem. **284** : 27176—27184, 2009.

23) Fukumoto, S., Kiba, T., Hall, B., Iehara, N., Nakamura, T., Longenecker, G., Krebsbach, P. H., Nanci, A., Kulkarni, A. B. and Yamada, Y. : Ameloblastin is a cell adhesion molecule required for maintaining the differentiation state of ameloblasts. J. Cell Biol. **167** : 973—983, 2004.

24) Dhamija, S. and Krebsbach, P. H. : Role of Cbfa1 in ameloblastin gene transcription. J. Biol. Chem. **276** : 35159—35164, 2001.

25) Nakamura, T., de Vega, S., Fukumoto, S., Jimenez, L., Unda, F. and Yamada, Y. : Transcription factor epiprofin is essential for tooth morphogenesis by regulating epithelial cell fate and tooth number. J. Biol. Chem. **283** : 4825—4833, 2008.

26) Diaz-Flores, L., Jr., Madrid, J. F., Gutierrez, R., Varela, H., Valladares, F., Alvarez-Arguelles, H. and Diaz-Flores, L. : Adult stem and transit-amplifying cell location. Histol. Histopathol. **21** : 995—1027, 2006.

27) Jarvinen, E., Salazar-Ciudad, I., Birchmeier, W., Taketo, M. M., Jernvall, J. and Thesleff, I. : Continuous tooth generation in mouse is induced by activated epithelial Wnt beta-catenin signaling. Proc. Natl.

Acad. Sci. USA **103** : 18627—18632, 2006.

28) Kuraguchi, M., Wang, X. P., Bronson, R. T., Rothenberg, R., Ohene-Baah, N. Y., Lund, J. J., Kucherlapati, M., Maas, R. L. and Kucherlapati, R. : Adenomatous polyposis coli (APC) is required for normal development of skin and thymus. PLoS Genet. **2** : e146, 2006.

29) Gat, U., DasGupta, R., Degenstein, L. and Fuchs, E. : De Novo hair follicle morphogenesis and hair tumors in mice expressing a truncated beta-catenin in skin. Cell **95** : 605—614, 1998.

30) Chu, E. Y., Hens, J., Andl, T., Kairo, A., Yamaguchi, T. P., Brisken, C., Glick, A., Wysolmerski, J. J. and Millar, S. E. : Canonical WNT signaling promotes mammary placode development and is essential for initiation of mammary gland morphogenesis. Development **131** : 4819—4829, 2004.

31) Liu, F., Thirumangalathu, S., Gallant, N. M., Yang, S. H., Stoick-Cooper, C. L., Reddy, S. T., Andl, T., Taketo, M. M., Dlugosz, A. A., Moon, R. T., Barlow, L. A. and Millar, S. E. : Wnt-beta-catenin signaling initiates taste papilla development. Nat. Genet. **39** : 106—112, 2007.

32) Thesleff, I., Vaahtokari, A. and Partanen, A. M. : Regulation of organogenesis. Common molecular mechanisms regulating the development of teeth and other organs. Int. J. Dev. Biol. **39** : 35—50, 1995.

THE JOURNAL OF BIOLOGICAL CHEMISTRY VOL. 285, NO 24, pp. 18948–18958, June 11, 2010
Printed in the U.S.A.

Pannexin 3 Regulates Intracellular ATP/cAMP Levels and Promotes Chondrocyte Differentiation*[S]

Received for publication, March 25, 2010 Published, JBC Papers in Press, April 19, 2010, DOI 10.1074/jbc.M110.127027

Tsutomu Iwamoto[‡§], Takashi Nakamura[‡§], Andrew Doyle[‡], Masaki Ishikawa[‡], Susana de Vega[‡], Satoshi Fukumoto[§], and Yoshihiko Yamada[‡1]

From the [‡]Laboratory of Cell and Developmental Biology, NIDCR, National Institutes of Health, Bethesda, Maryland 20892-4370 and the [§]Department of Pediatric Dentistry, Tohoku University Graduate School of Dentistry, Sendai 980-8576, Japan

Pannexin 3 (Panx3) is a new member of the gap junction pannexin family, but its expression profiles and physiological function are not yet clear. We demonstrate in this study that Panx3 is expressed in cartilage and regulates chondrocyte proliferation and differentiation. *Panx3* mRNA was expressed in the prehypertrophic zone in the developing growth plate and was induced during the differentiation of chondrogenic ATDC5 and N1511 cells. Panx3-transfected ATDC5 and N1511 cells promoted chondrogenic differentiation, but the suppression of endogenous Panx3 inhibited differentiation of ATDC5 cells and primary chondrocytes. Panx3-transfected ATDC5 cells reduced parathyroid hormone-induced cell proliferation and promoted the release of ATP into the extracellular space, possibly by action of Panx3 as a hemichannel. Panx3 expression in ATDC5 cells reduced intracellular cAMP levels and the activation of cAMP-response element-binding, a protein kinase A downstream effector. These Panx3 activities were blocked by anti-Panx3 antibody. Our results suggest that Panx3 functions to switch the chondrocyte cell fate from proliferation to differentiation by regulating the intracellular ATP/cAMP levels.

Cartilage plays an important role in mechanical load resistance and in skeletal structure support. It also serves as the skeletal template for endochondral ossification by which most bones in the body, such as long bones, are formed. In endochondral ossification, cartilage development is initiated by mesenchymal cell condensation, followed by a series of proliferation and differentiation processes. Cells undergoing condensation differentiate into chondrocytes, which then proliferate, produce type II collagen and form the proliferative zone of the cartilage molds. As development proceeds, chondrocytes in the center of the cartilage molds (prehypertrophic zone) cease proliferating and differentiate into type X collagen-producing hypertrophic chondrocytes to form the hypertrophic zone. Terminally differentiated hypertrophic chondrocytes mineralize the surrounding matrix. Eventually these cells die by apoptosis and are replaced by osteoblasts that form trabecular bone.

The regulation of chondrocyte proliferation and differentiation must be tightly coordinated to allow formation of properly sized cartilage and bone (1). Parathyroid hormone-related peptide (PTHrP)[2] and parathyroid hormone (PTH) sustain chondrocyte proliferation and delay differentiation of the growth plate (2). PTHrP is expressed by perichondrial cells and chondrocytes in the upper region of growing cartilage. Mutant mice that are deficient in PTHrP (3), PTH (4), or its receptor (5) have short proliferative zones and accelerated chondrocyte differentiation, which results in abnormal endochondral bone formation. In contrast, mice that overexpress PTHrP have enlarged proliferative zones and delayed chondrocyte terminal differentiation (6). Humans with an activating mutation in the PTH/PTHrP receptor develop Jansen metaphyseal chondrodysplasia, characterized by disorganization of the growth plates and delayed chondrocyte terminal differentiation (7). These results suggest that PTH/PTHrP signaling regulates skeletal development by promoting cell proliferation and inhibiting hypertrophic differentiation of chondrocytes.

The binding of PTH/PTHrP to its receptor activates both G_s and G_q family heterotrimeric G proteins (8, 9). The activation of G_s is necessary for cAMP production and protein kinase A (PKA) activation, which leads to phosphorylation of the cAMP-response element-binding (CREB) family of transcription factors. CREB then induces genes such as the cyclin D1 and cyclin A genes. The activated cyclin/cyclin-dependent kinases in turn phosphorylate the retinoblastoma protein and its relative factors, which then dissociates the E2F transcription factor and subsequently activates the target genes necessary for DNA replication and cell cycle progression. Thus, CREB is a direct target of PKA and a downstream target of PTH/PTHrP/cAMP signaling and is required for chondrocyte proliferation (10, 11). How proliferation signaling is down-regulated in the prehypertrophic zone to stop proliferation and allow the switch to the postmitotic state is not well understood.

Pannexins, relatives of innexins that had been considered as exclusively invertebrate gap junction proteins, were recently

* This work was supported, in whole or in part, by a National Institutes of Health grant from Intramural Research Program of NIDCR (to Y. Y.). This work was also supported by Grant-in-aid for Research Fellows 20791583 from the Japan Society for the Promotion of Science (to T. I.) and Grant-in-aid from the Ministry of Education, Science, and Culture of Japan 20679006 (to S. F.).

[S] The on-line version of this article (available at http://www.jbc.org) contains supplemental Fig. 1.

[1] To whom correspondence should be addressed: Bldg. 30, Rm. 407, NIDCR, National Institutes of Health, 30 Convent Dr., MSC 4370, Bethesda, MD 20892-4370. Tel.: 301-496-2111; Fax: 301-402-0897; E-mail: yoshi.yamada@nih.gov.

[2] The abbreviations used are: PTHrP, parathyroid hormone-related peptide; PTH, parathyroid hormone; PKA, protein kinase A; CREB, cAMP-response element-binding protein; ER, endoplasmic reticulum; RT, reverse transcription; shRNA, short hairpin RNA; siRNA, short interfering RNA; MAPK, mitogen-activated protein kinase; TES, 2-{[2-hydroxy-1,1-bis(hydroxymethyl)ethyl]amino}ethanesulfonic acid.

discovered as candidates for a second family of gap junction proteins in vertebrates (12). Although there are some similarities in domain structures between pannexins and connexins, which are well characterized as vertebrate gap junction proteins, these two protein families have no sequence homology (13). The pannexin family has three members as follows: pannexin 1 (Panx1), pannexin 2 (Panx2), and pannexin 3 (Panx3). These proteins were originally identified in the human and mouse genomes (12). The expression of Panx1 is observed in many organs, such as the eye, thyroid, prostate, kidney, and liver, but its expression is especially strong in both the developing and mature central nervous system (12–14). Panx2 is preferentially expressed in the central nervous system. Recently, it was reported that Panx3 is expressed in skin, cartilage, and cochlea (15–17).

In *Xenopus* oocytes, Panx1 forms both nonjunctional hemichannels and intercellular channels and interacts with Panx2 (18). Panx1 hemichannels are stress-sensitive conduits for ATP (19). Panx1 is a Ca^{2+}-permeable ion channel that is localized on both the ER and plasma membrane and participates in ER Ca^{2+} leakage and intercellular Ca^{2+} movement (20). Both Panx1 and Panx3 are glycoproteins, and *N*-glycosylation of these pannexins plays a role in intracellular trafficking and functional channel function (15, 16). The physiological function of pannexins in cell differentiation has not yet been characterized however.

In this study, we report that Panx3 regulates the proliferation and differentiation of chondrocytes. *Panx3* mRNA was expressed in prehypertrophic chondrocytes and induced during the differentiation of chondrogenic ATDC5 cells. The transfection of Panx3 into ATDC5 cells promoted ATDC5 cell differentiation, whereas the inhibition of endogenous Panx3 by shRNA blocked differentiation. Panx3 promoted ATP release into the extracellular space and inhibited PTH-mediated cell proliferation, intracellular levels of cAMP, and phosphorylation of CREB. Thus, our results suggest that Panx3 regulates the transition of proliferation to differentiation in chondrocytes.

EXPERIMENTAL PROCEDURES

Reagents—Insulin/transferrin/sodium selenite (ITS) was obtained from Sigma. Recombinant rat PTH(1–34) was purchased from Bachem. Recombinant human BMP2 was purchased from Humanzyme.

In Situ Hybridization—Digoxigenin-11-UTP-labeled, single-stranded antisense RNA probes for *Panx3*, *Ihh*, *Col2a1*, *Col10a1*, and *Hist1h4c* were prepared using the DIG RNA labeling kit (Roche Applied Science) according to the manufacturer's instructions. *In situ* hybridization of the tissue sections was performed essentially according to the protocol provided with Link-Label ISH core kit (Biogenex). Frozen tissue sections from growth plates (E16.5) were generated and placed on RNase-free glass slides. After drying the frozen sections for 10 min at room temperature and incubating at 37 °C for 30 min, the sections were treated with 10 μg/ml proteinase K at 37 °C for 30 min. Hybridization was performed at 37 °C for 16 h, and washes were carried out with 2× SSC at 50 °C for 15 min and 2× SSC containing 50% formamide at 37 °C for 15 min. The slides were then subjected to digestion with 10 μg/ml RNase A in 10 mM Tris-HCl (pH 7.6), 500 mM NaCl, and 1 mM EDTA at 37 °C for 15 min and then washed. The sections were treated with 2.4 mg/ml Levamisole (Sigma) to inactivate endogenous alkaline phosphatase.

Antibody for Panx3—A rabbit polyclonal antibody to a peptide (amino acid residues, HHTQDKAGQYKVKSLWPH) from the first extracellular loop of the mouse Panx3 protein was prepared. The antiserum was purified by the peptide affinity column. This purified antibody reacts specifically to Panx3 and was used for immunohistochemistry, Western blotting, and functional blocking assay. For inhibition by the Panx3 antibody, the cells were incubated with 10 ng/ml affinity-purified antibody or control IgG for 30 min before the experiments. To abrogate the blocking activity with Panx3 antibody, the Panx3 peptide was preincubated with the Panx3 antibody. A peptide with a scrambled sequence (WHTKYQVGLDPQHKASHK) of the Panx3 peptide was used as a control.

Immunohistochemistry—Frozen tissue sections were fixed with acetone at −20 °C for 2 min and treated with liberate antibody binding solution for 15 min at 37 °C. For cultured cell staining, the cells were fixed with acetone at −20 °C for 2 min. Immunohistochemistry was performed on sections that were incubated with Universal Blocking Reagent (Biogenex) for 7 min at room temperature before incubation with the primary antibody. The primary antibodies were detected by Cy-3- or Cy-5-conjugated secondary antibodies (Jackson ImmunoResearch). Nuclear staining was performed with Hoechst dye (Sigma). A fluorescence microscope (Axiovert 200; Carl Zeiss MicroImaging, Inc.) and 510 Meta confocal microscope (Zeiss) were used for immunofluorescent image analysis. For green fluorescent protein and ER-Tracker Red (Invitrogen) staining, ATDC5 cells were transfected for 2 days and then stained with ER-Tracker Red as described in the manufacturer's instructions. The images were prepared with AxioVision and Photoshop (Adobe Systems, Inc.).

Cell Culture—ATDC5 cells (21) were grown in Dulbecco's modified Eagle's medium/F-12 (Invitrogen) containing 5% fetal bovine serum (HyClone) and under 5% CO_2. In proliferation conditions, cells were maintained under confluency, and the media were replaced every other day. In differentiation conditions, cells were plated in confluency and incubated in the same medium plus 10 μg/ml insulin, 10 μg/ml transferrin, and 10 μg of selenium. N1511 cells (22) were cultured with α-minimal essential medium (Invitrogen) containing 2% fetal bovine serum (HyClone) under 5% CO_2. As differentiation conditions, 1 μM insulin, 100 ng/ml rhBMP2, and 50 μg/ml ascorbic acid were added in the culture medium.

Mouse primary chondrocytes were isolated from neonatal ICR mice as described previously (23). Distal cartilaginous ends of femurs and humeri were digested with 0.25% trypsin, 0.01% EDTA for 15 min, followed by digestion with 2 mg/ml collagenase type I (Worthington) in Dulbecco's modified Eagle's medium/F-12 overnight. Neonatal mouse cartilage tissue was dispersed by pipetting, and cells were filtered through 100-μm cell strainers (Falcon). Single cells were inoculated onto type I collagen-coated multiwell dishes maintained in 10% fetal bovine serum in α-minimal essential medium.

RT-PCR and Real Time PCR—Total RNA was extracted from cells using the TRIzol reagent kit (Invitrogen). Two μg of total RNA was used for reverse transcription to generate cDNA, which was used as a template for PCR with gene-specific primers. Each cDNA was amplified with an initial denaturation at 95 °C for 3 min; then 95 °C for 30 s, 60 °C for 30 s, and 72 °C for 30 s for 25 cycles; and a final elongation step at 72 °C for 5 min and then separated on agarose gels. Real time PCR was performed with SYBR Green PCR master mix and the TaqMan 7700 sequencer detection system (Applied Biosystems). PCR was performed for 40 cycles as follows: 95 °C for 1 min, 60 °C for 1 min, and 72 °C for 1 min. Gene expression was normalized to the housekeeping gene *S29*. The reactions were run in triplicate and repeated three times, and the results were combined to generate the graphs. The following primer sequences were used: *Panx3*, 5′-GCCCCTGGATAAGATGGTCAAG-3′ and 5′-GCGGATGGAACGGTTGTAAGA-3′; *Panx1*, 5′-TTTGGACCTAAGAGACGGACCTG-3′ and 5′-CGGGAATCAGCAGAGCATACAC-3′; *Panx2*, 5′-ACAAGGGCAGTGGAGGTGATTC-3′ and 5′-CGATGAGGATAGCGTGCTGATG-3′; *Col2a1*, 5′-GAAAAACTGGTGGAGCAGCAAGAGC-3′ and 5′-CAATAATGGGAAGGCGGGAGGTC-3′; *Agc1*, 5′-TGGAGCATGCTAGAACCCTCG-3′ and 5′-GCGACAAGAAGACACCATGTG-3′; *Col10a1*, 5′-AGCCCCAAGACACAATACTTCATC-3′ and 5′-TTTCCCCTTTCCGCCCATTCACAC-3′; *PPR*, 5′-ACTACTACTGGATTCTGGTGGAGGG-3′ and 5′-CTGGAAGGAGTTGAAGAGCATCTC-3′; *PTHrP*, 5′-CAGACGATGAGGGCAGATACCTAAC-3′ and 5′-CAGTTTCCTGGGGAGACAGTTTG-3′; and *Gapdh*, 5′-ACCACAGTCCATGCCATCAC-3′ and 5′-TCCACCACCCTGTTGCTGTA-3′. The predicted size of each fragment is 373, 380, 442, 392, 325, 463, 470, 558, 470, 372, and 452 bp.

Western Blotting—The cells were washed three times with phosphate-buffered saline containing 1 mM sodium vanadate (Na_3VO_4) and then solubilized in 100 μl of lysis buffer (10 mM Tris-HCl (pH 7.4), 150 mM NaCl, 10 mM $MgCl_2$, 0.5% Nonidet P-40, 1 mM phenylmethylsulfonyl fluoride, and 20 units/ml aprotinin). Lysed cells were centrifuged at 14,000 rpm for 30 min, and the protein concentration of each sample was measured with Micro-BCA assay reagent (Pierce). The samples were denatured in SDS sample buffer and loaded onto a 12% SDS-polyacrylamide gel. Ten μg of lysate protein was applied to each lane. After SDS-PAGE, the proteins were transferred onto a polyvinylidene difluoride membrane and immunoblotted with anti-CREB, anti-phospho-CREB (Cell Signaling Technology, Inc.), anti-MAPK, and anti-phospho-MAPK (New England Biolabs) and then visualized using an ECL kit (Amersham Biosciences). For CREB and ERK1/2 experiments, the cells were pretreated as follows. The cells (3×10^4 cell/cm^2) were plated in a 60-mm dish and cultured with 10 μg/ml insulin, 10 μg/ml transferrin, and 10 μg of selenium for 7 days. They were incubated with serum-free 0.1% albumin-containing Dulbecco's modified Eagle's medium/F-12 medium for 8–12 h and then exposed to 100 nM rPTH(1–34) for the appropriate times.

Plasmid Construction and Transfection—The coding sequence of mouse Panx3 cDNA was subcloned into the pEF1/V5-His vector (pEF1/Panx3) and pcDNA3.1-GFP-TOPO (Panx3-pcDNA-GFP) (Invitrogen). As a control, an empty vector of pEF1 or pcDNA3.1-GFP-TOPO was used. ATDC5 cells or N1511 cells were transiently transfected using Nucleofector (Amaxa). Briefly, cells were resuspended in 100 μl of Nucleofector solution T and transfected with 5 μg of DNA using Program T-20. Transfection efficiency using these conditions was shown to be >70%. For stable transfection of ATDC5 cells, selection was initiated 24 h after transfection using G418 (Invitrogen) at a concentration of 600 μg/ml for 2 weeks. Pools of transfected cells were collected and cultured as the parental ATDC5 cells, in the continued presence of 60 μg/ml G418. All experiments were performed three times, and representative experiments are shown. For transient transfection, Panx3-pcDNA-GFP was transfected into ATDC5 cells under the same conditions as used for stable transfection, except that G418 was omitted.

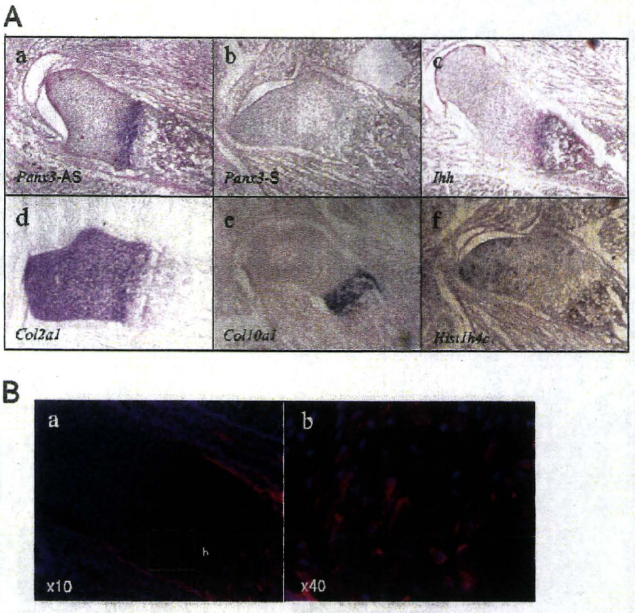

FIGURE 1. **Expression of Panx3 in E16.5 growth plates.** *A, in situ* hybridization. Panx3 mRNA was expressed in prehypertrophic chondrocytes, perichondrium, and osteoblasts. The following are shown: antisense *Panx3* (*panel a*); sense *Panx3* (*panel b*); *Ihh* (*panel c*); *Col2a1* (*panel d*); Col10a1 (*panel e*); and *Hist1h4c* (*panel f*). *B*, immunostaining with anti-Panx3 antibody (*red*) and Hoechst nuclear staining (*blue*). A magnified view of the areas (*panel a*) is marked by the *square* in *panel b*.

Alcian Blue Staining—The cells were first rinsed with phosphate-buffered saline three times and then fixed with 100% methanol for 10 min at −20 °C. Staining was accomplished by applying a solution of 0.1% Alcian blue 8 GX in 0.1 M HCl to the cells for 2 h at room temperature. To quantify the intensity of the staining, the stained culture plates were rinsed with phosphate-buffered saline three times, and the well was extracted with 6 M guanidine HCl for 8 h at room temperature. The absorbance of the extracted dye was measured at 650 nm.

Short Hairpin RNA Experiments—Panx3-specific knockdowns were performed with the expression of shRNA using a pSM2 vector (Open Biosystems). The shRNA construct contains the 3′-untranslated region of *Panx3* (GGCAGGGTAGAACAATTTA). A nonsilencing shRNA construct from Open Biosystems, whose sequence has been verified to contain no homology to known mammalian genes, was used as a control. The cells were transfected with shRNA plasmids using

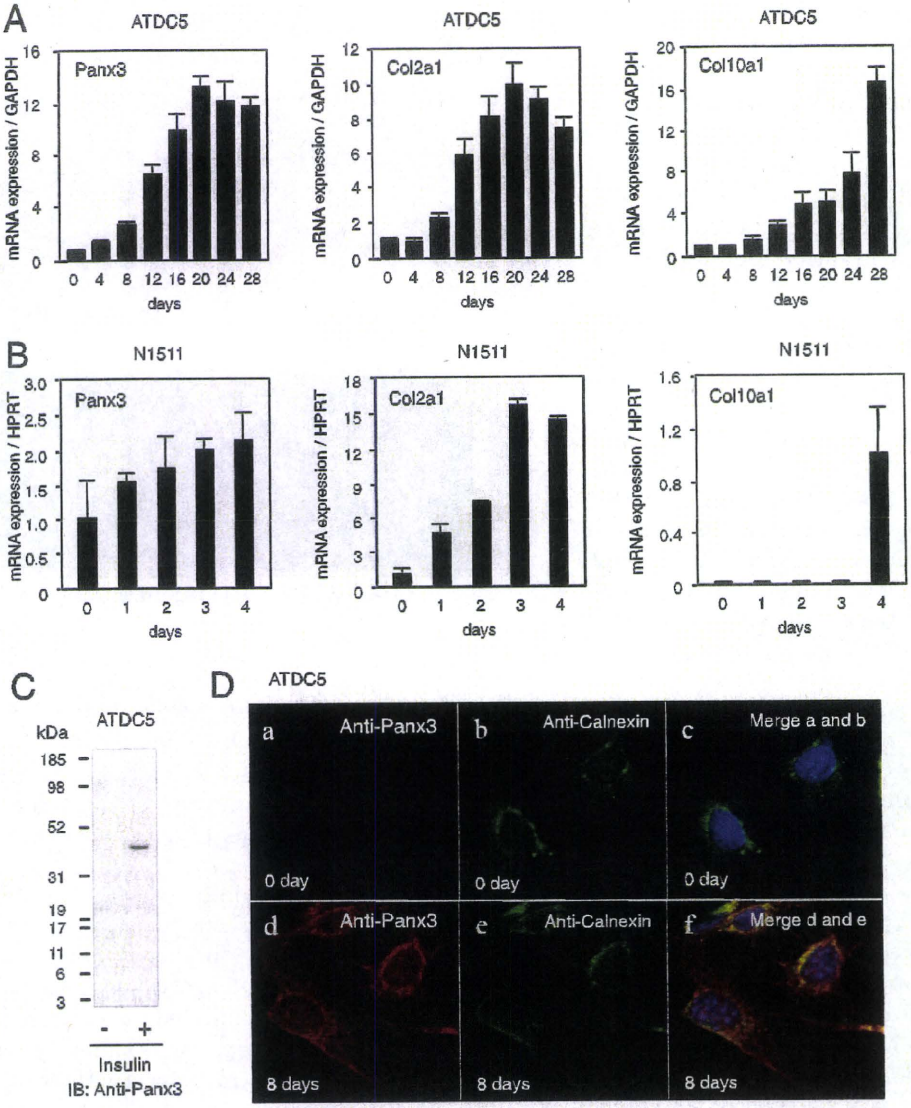

FIGURE 2. **Expression of Panx3 in differentiating ATDC5 and N1511 cells.** *A*, mRNA expression in differentiating ATDC5 cells. ATDC5 cells were cultured with 10 μg/ml insulin. Total RNA was extracted from cells on the indicated days after insulin treatment and analyzed with real time RT-PCR. In differentiating ATDC5 cells, *Panx3*, *Col2a1*, and *Col10a1* were strongly induced. *GAPDH*, glyceraldehyde-3-phosphate dehydrogenase, was used as a control. *B*, mRNA expression in differentiating N1511 cells. N1511 cells were cultured with 1 μM insulin, 100 ng/ml rhBMP-2, and 50 μg/ml ascorbic acid for differentiation. Panx3 was also progressively induced in differentiating N1511 cells. *HPRT*, hypoxanthine phosphoribosyltransferase, was used as a control. *C*, expression of Panx3 protein in undifferentiated (*1st lane*) and differentiated ATDC5 cells (*2nd lane*). ATDC5 cells were treated with or without insulin for 20 days, and cell extracts were analyzed by Western blotting using Panx3 antibody. Panx3 protein was induced in differentiated ATDC5 cells. *IB*, immunoblot. *D*, immunostaining with anti-Panx3 antibody (*red*), ER marker (*green*), calnexin, and Hoechst nuclear staining (*blue*). In differentiating ATDC5 cells, endogenous Panx3 was observed in the cell membrane, cell processes, and ER (*panels d–f*) but not in undifferentiated cells (*panels a* and *c*).

Nucleofection (Amaxa). Selection was performed 24 h after transfection with puromycin at a concentration of 4 μg/ml for 5 days.

siRNA Experiments—siRNAs targeting mouse Panx3 (NM_172454) (Panx3 siRNA-1, 5′-UAAUAAGGAUGUCCACGUA-3′ and Panx3 siRNA-2, 5′-GGGCUCAGAUUAUGGACUA-3′) were purchased from Dharmacon (siGenome On-Target Plus; Dharmacon). Negative control siRNA duplex (Stealth RNAi negative control; Invitrogen) was used as control. Forward transfection for ATDC5 cells and reverse transfection for primary chondrocytes were carried out using Lipofectamine RNAiMAX reagent (Invitrogen), according to the manufacturer's protocol. In forward transfection, ATDC5 cells were transfected with 50 nM siRNA duplex in regular serum-free culture medium without antibiotics, using Lipofectamine RNAiMAX reagent. After 8 h of incubation with the transfection reagent mixture, the medium was changed to the differentiation medium with BMP-2 and incubated for 8 days. In reverse transfection, freshly isolated chondrocytes were plated at an initial density of 5×10^4/cm^2, into the plates that had been coated with Panx3 siRNA-1, siRNA-2, or Stealth RNAi negative control in the presence of Lipofectamine RNAiMAX reagent. After 8 h of incubation with the transfection reagent mix, the medium was changed to the differentiation medium with BMP-2 and incubated for 2 days. Expressions of *Panx3*, *Col2a1*, and *Col10a1* were analyzed by real time PCR methods.

Measurement of Intracellular cAMP—The cells were seeded at 1×10^4 cells/well in a 96-well plate and cultured for 7 days with Dulbecco's modified Eagle's medium/F-12 in the presence of 10 μg/ml of ITS. They were then incubated with serum-free 0.1% albumin containing Dulbecco's modified Eagle's medium/F-12 medium for 8–12 h, followed by exposure to 100 nM rPTH(1–34) for 10 min. The level of cAMP was determined with a Bridge-It cAMP Designer fluorescence assay kit (Mediomics). Briefly, the cells were incubated with 50 μl of 1× Krebs-Ringer/isobutylmethylxanthine buffer for 15 min at room temperature and with 50 μl of forskolin for 15 min at room temperature. After the solution was removed, the cells were incubated with 100 μl of the cAMP designer assay solution for 30 min while covered with aluminum foil to avoid exposure to light. The supernatant was collected, and the fluorescence intensity was measured with a plate reader (excitation, ~480–485 nm; emission, ~520–535 nm).

Measurement of ATP Flux—ATP flux was determined by luminometry. To open the pannexin channels, the cells were depolarized by incubation in KGlu solution (140 mM KGlu, 10 mM KCl, and 5.0 mM TES, pH 7.5) for 10 min. The super-

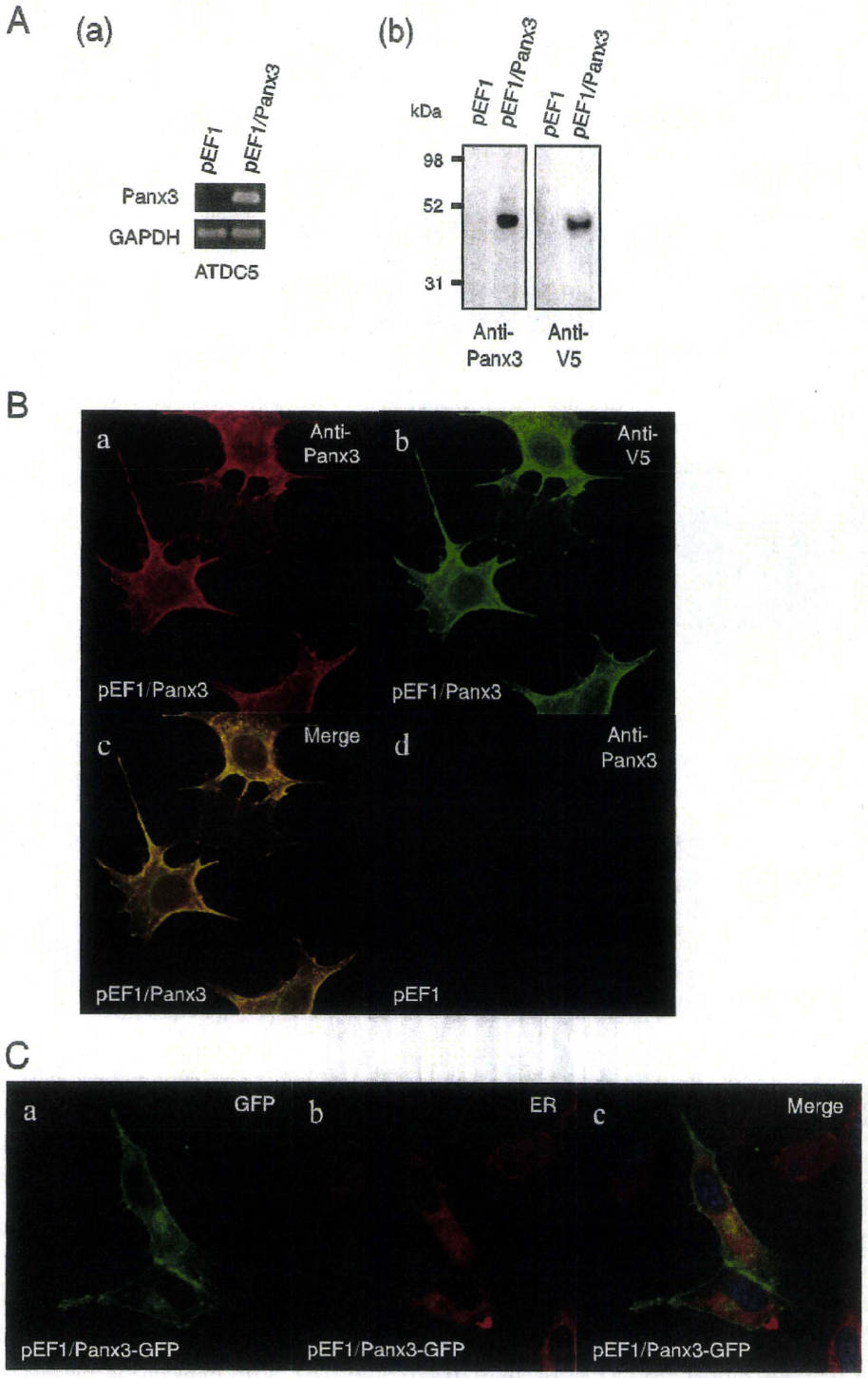

FIGURE 3. **Panx3 expression in Panx3-transfected ATDC5 cells.** ATDC5 cells were stably transfected with the control empty vector (*pEF1*) or the Panx3 expression vector (*pEF1/Panx3*). *A*, expression of Panx3 mRNA and protein. Pooled transfectants were analyzed by RT-PCR (*panel a*) and Western blotting (*panel b*) using anti-Panx3 and anti-V5 antibodies. *GAPDH*, glyceraldehyde-3-phosphate dehydrogenase. *B*, immunostaining of Panx3-transfected ATDC5 cells using anti-Panx3 (*red*) and anti-V5 (*blue*) antibodies. Fluorescent confocal images showed that the staining signals of Panx3 and V5 antibodies were co-localized in the cell membrane, cell-cell junction, and organelles. No staining of either Panx3 or V5 antibodies was observed in control pEF1-transfected ATDC5 cells. *C*, co-localization of Panx3-GFP and ER-Tracker Red. ATDC5 cells were transiently transfected with Panx3-pcDNA-GFP or pcDNA3.1-GFP-TOPO (control) for 2 days. Panx3-GFP was co-localized with ER-Tracker Red, indicating the presence of Panx3 in ER. *GFP*, green fluorescent protein.

natant was collected and assayed with luciferase/luciferin (Promega).

RESULTS

Expression of Panx3 in Cartilage—While searching for an expression profile of gap junction genes in skeletal tissues through the EST data base, we found that *Panx3* was expressed in limbs and cartilage. Because of its unique expression profile and its potential function in skeletal development, we characterized the expression and function of Panx3 in cartilage. *In situ* hybridization of the embryonic day (E) 16.5 growth plates revealed that *Panx3* mRNA was strongly expressed in the prehypertrophic zone (Fig. 1*A*, *panel a*). A control sense probe for *Panx3* showed no signal (Fig. 1*A*, *panel b*). Indian hedgehog (*Ihh*) mRNA was expressed in prehypertrophic and hypertrophic chondrocytes at this stage (Fig. 1*A*, *panel c*). mRNA for type II collagen (*Col2a1*), a major collagen in cartilage, was expressed in the resting, proliferative, and prehypertrophic zones (Fig. 1*A*, *panel d*). Type X collagen (*Col10a1*) mRNA was expressed in the prehypertrophic and hypertrophic chondrocyte chondrocytes (Fig. 1*A*, *panel e*). Histone H4 (*Hist1h4c*), a marker for cell proliferation, was expressed in proliferating chondrocytes (Fig. 1*A*, *panel f*). Immunostaining with a Panx3 antibody showed that Panx3 protein was expressed in prehypertrophic and hypertrophic chondrocytes and was localized on the surface of these cells (Fig. 1*B*). Panx3 was also expressed in perichondrial cells and osteoblasts.

Expression of Panx3 in Differentiating Chondrogenic Cells—The expression of *Panx3* mRNA in a transitional stage between proliferative and hypertrophic chondrocytes suggests that Panx3 regulates chondrocyte proliferation and differentiation. To assess the role of Panx3 in chondrocyte differentiation, we used the murine chondrogenic cell lines ATDC5 and N1511, which are used to study multistep processes of

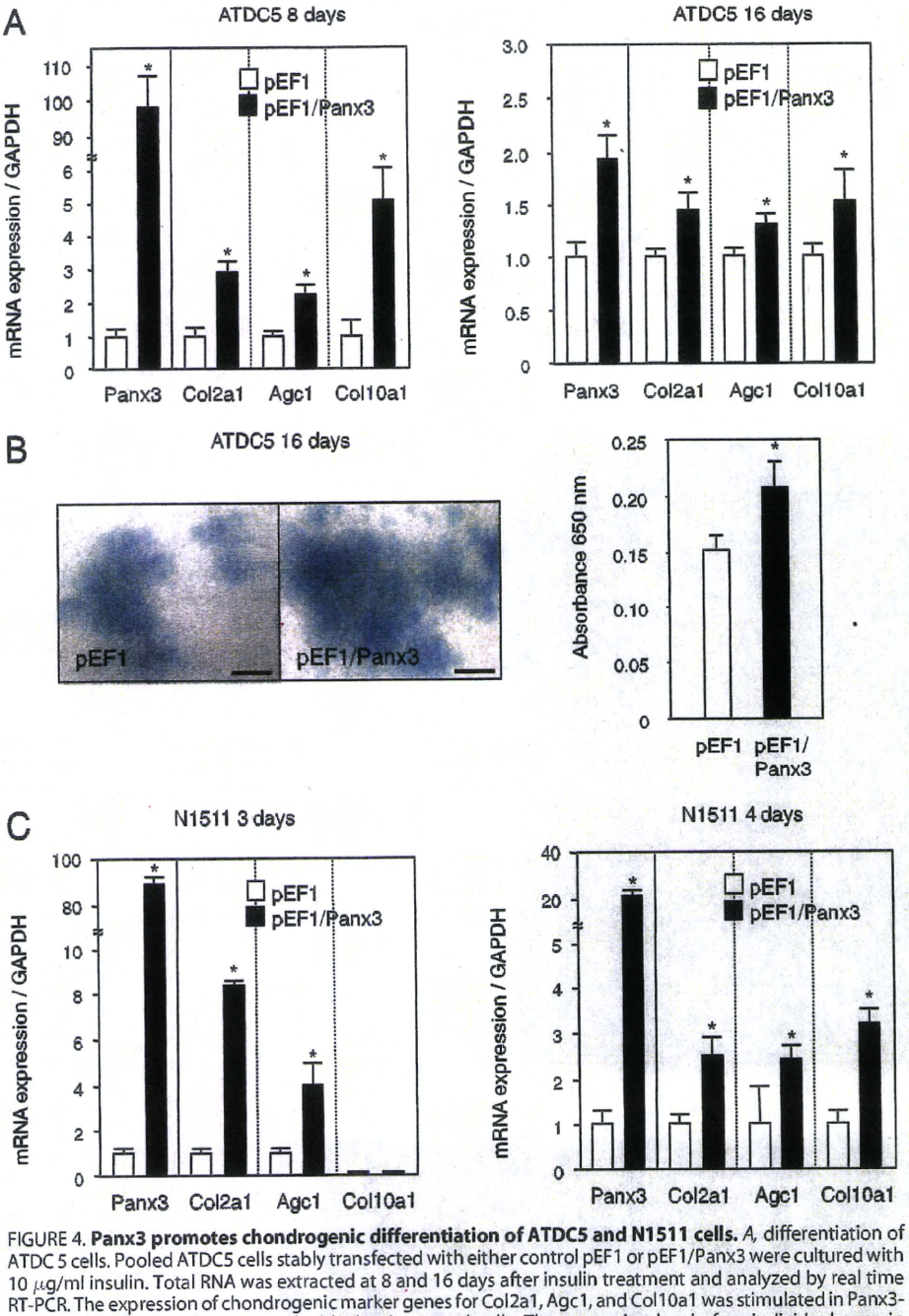

FIGURE 4. **Panx3 promotes chondrogenic differentiation of ATDC5 and N1511 cells.** *A*, differentiation of ATDC 5 cells. Pooled ATDC5 cells stably transfected with either control pEF1 or pEF1/Panx3 were cultured with 10 μg/ml insulin. Total RNA was extracted at 8 and 16 days after insulin treatment and analyzed by real time RT-PCR. The expression of chondrogenic marker genes for Col2a1, Agc1, and Col10a1 was stimulated in Panx3-transfected ATDC5 cells compared with that in control cells. The expression level of an individual gene in control pEF1-transfected cells was set as 1.0, and we compared it with the level of each gene in Panx3-transfected cells for each day 8 and 18. The exogenous Panx3 levels were the same but endogenous Panx3 levels were strongly increased from day 8 to 16. As results, the ratio at day 16 was less than that in day 8. *GAPDH*, glyceraldehyde-3-phosphate dehydrogenase. *B*, Alcian blue staining of ATDC5 cells. After 16 days of culture, Alcian blue staining was performed. Alcian blue staining was increased in Panx3-transfected ATDC5 cells compared with that in pEF1-transfected ATDC5 cells. *Scale bar*, 200 μm. *C*, differentiation of N1511 cells. N1511 cells were transfected with either control pEF1 or pEF1/Panx3, were cultured with 1 μM insulin, 100 ng/ml rhBMP-2, and 50 μg/ml ascorbic acid for 3 s and 4 days. Similar to the results of ATDC5 cells, chondrogenic maker genes expression was stimulated by Panx3. Statistical analysis was performed using analysis of variance (*, $p < 0.01$).

chondrocyte differentiation (21, 22). ATDC5 cells proliferate until confluency and then differentiate into chondrocytic phenotypes in a prolonged culture in the presence of insulin (21). Factors such as BMP-2, GDF-5, and transforming growth factor β accelerate the chondrogenic differentiation of ATDC5 cells (24–26). We first examined the expression of *Panx3* mRNA during differentiation of the ATDC5 cells in the presence of insulin using real time RT-PCR (Fig. 2*A*). *Panx3* mRNA expression was induced during ATDC5 cell differentiation and reached its highest level after 20 days of culture (Fig. 2*A*). The expression of *Col2a1* mRNA was increased in a similar manner to that of *Panx3* mRNA; *Col10a1* mRNA was induced at later stages of differentiation. Without insulin, the induction of *Panx3*, *Col2a1*, and *Col10a1* was low even in a prolonged culture, indicating that *Panx3* expression was clearly linked to the differentiation of ATDC5 cells. We observed similar expression patterns in those genes during BMP-2-induced ATDC5 differentiation, except that BMP-2 promoted differentiation much faster than insulin (data not shown). In another chondrogenic cell line N1511, BMP-2- and insulin-induced expressions of *Panx3*, *Col2a1*, and *Col10a1* were seen (Fig. 2*B*). Western blot analysis demonstrated that Panx3 protein with a molecular mass of 45 kDa was induced in differentiated ATDC5 cells (Fig. 2*C*). These results indicate that Panx3 was induced during chondrogenic differentiation of ATDC5 and N1511 cells.

Membrane Localization of Panx3 in ATDC5 Cells—To examine cellular localizations of Panx3, we immunostained differentiated ATDC5 cells using anti-Panx3 antibody (Fig. 2*D*). Panx3 was expressed in the plasma membrane, cell extensions, and in organelles most likely found in the ER and the Golgi of ATDC5 cells 8 days after differentiation induction. Panx3 was co-localized with calnexin, an ER marker, indicating that the localization of Panx3 was most likely in the ER (Fig. 2*D*, *panels d* and *e*). There was no staining signal for Panx3 in undifferentiated ATDC5 cells (Fig. 2*D*, *panel a*). We also examined the expression and localization of Panx3 in pooled, stable Panx3-transfected ATDC5 cells (Fig. 3, *A* and *B*). In these cells, Panx3 mRNA and protein were strongly expressed in an undifferentiated condition. Both anti-Panx3 and anti-V5 antibodies

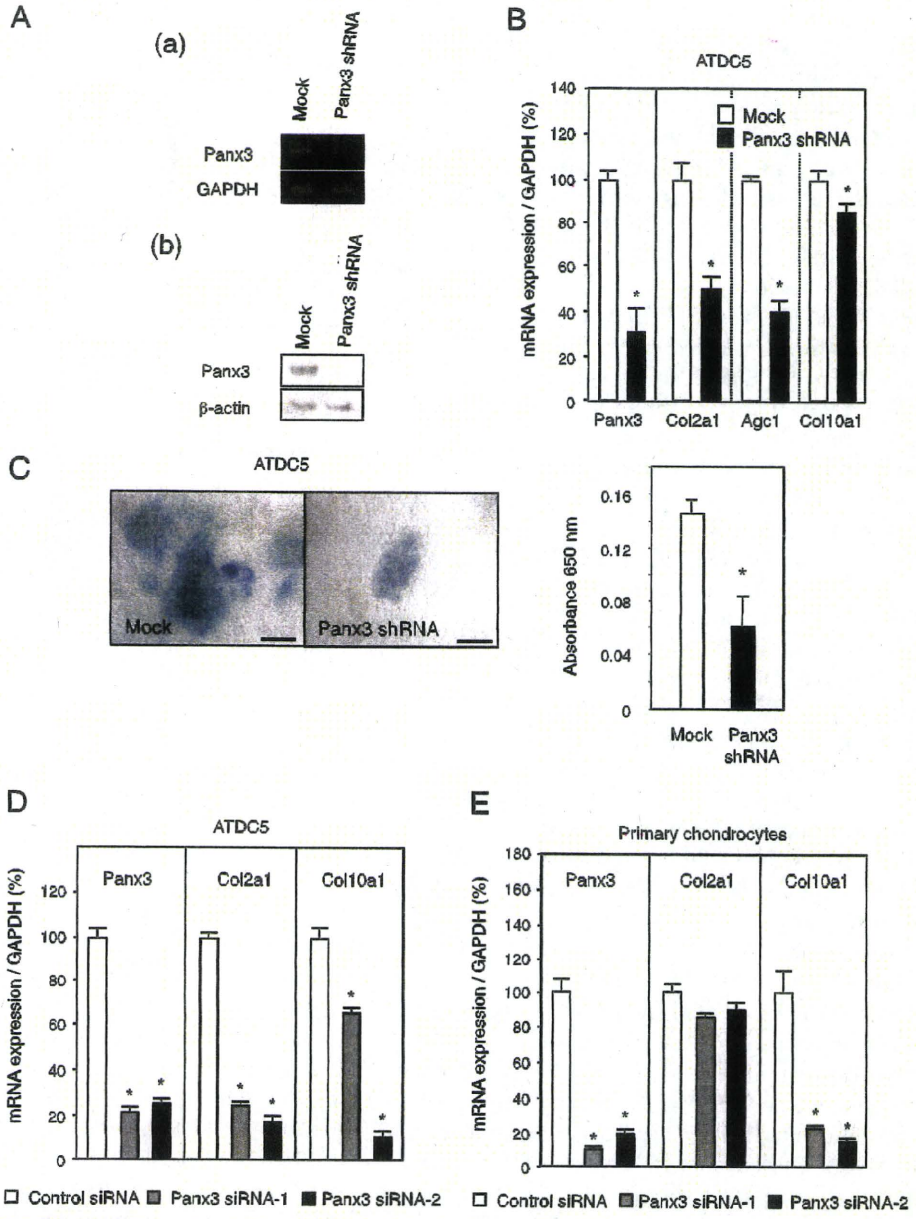

FIGURE 5. **Inhibition of ATDC5 cell differentiation by Panx3 shRNA.** Pooled ATDC5 cells stably transfected with either control vector (*Mock*) or Panx3 shRNA vector were cultured with 10 μg/ml insulin. *A*, reduced expression of endogenous Panx3. Total RNA and protein were prepared from cells after 8 days of culture and analyzed through RT-PCR (*panel a*) and Western blotting (*panel b*), using anti-Panx3 antibody. Panx3 expression was reduced in Panx3 shRNA-transfected ATDC5 cells. *GAPDH*, glyceraldehyde-3-phosphate dehydrogenase. *B*, reduced expression of chondrogenic marker genes. Total RNA was prepared from cells after 8 days of culture and analyzed by real time RT-PCR. Expression of *Col2a1*, *Agc1*, and *Col10a1* was reduced in Panx3 shRNA-transfected ATDC5 cells. *C*, Alcian blue staining. After 16 days of culture, Alcian blue staining was performed. Alcian blue staining was reduced in Panx3 shRNA-transfected cells. *Scale bar*, 200 μm. Statistical analysis was performed using analysis of variance (*, $p < 0.01$). *D*, reduced expression of *Col2a1* and *Col10a1* by Panx3 siRNA in ATDC5 cells. ATDC5 cells transfected with control siRNA, Panx3 siRNA-1, or Panx3 siRNA-2 were cultured with 100 ng/ml BMP-2 for 8 days. Expressions of *Panx3*, *Col2a1*, and *Col10a1* were analyzed by real time PCR methods. Expression of *Col2a1* and *Col10a1* was reduced in Panx3 siRNA-transfected ATDC5 cells. *E*, reduced expression of *Col10a1* but not *Col2a1* by Panx3 siRNA in primary chondrocytes. Primary chondrocytes transfected with control siRNA, Panx3 siRNA-1, or Panx3 siRNA-2 were cultured with 100 ng/ml BMP-2 for 2 days. Expressions of *Panx3*, *Col2a1*, and *Col10a1* were analyzed by real time PCR methods. Expression of *Panx3* and *Col10a1*, but not *Col2a1*, was reduced in Panx3 siRNA-transfected primary chondrocytes. Statistical analysis was performed using analysis of variance (*, $p < 0.01$).

detected the recombinant protein as a single band of about 49 kDa, corresponding to the predicted molecular weight of the Panx3-V5-His fusion protein (Fig. 3*A*). The immunohistochemistry of Panx3-transfected ATDC5 cells showed that both anti-Panx3 and anti-V5 antibodies strongly stained the plasma membranes (Fig. 3*B*). Some Panx3 signals were also observed in the ER because ER-Tracker Red, which had been transiently transfected with the Panx3 expression vector containing a green fluorescent protein tag, revealed that Panx3 was co-localized with an ER marker. This indicates that the localization of Panx3 was most likely in the ER (Fig. 3*C*).

Panx3 Promotes ATDC5 and N1511 Cell Differentiation—We next examined whether the overexpression of Panx3 affects ATDC5 cell differentiation. Panx3-transfected ATDC5 cells were cultured under the differentiation condition in the presence of insulin. The expression of chondrocyte marker genes for *Col2a1*, aggrecan (*Agc1*), and *Col10a1* increased by 2.8-, 2.2-, and 5.1-fold, respectively, compared with control pEF1-transfected cells 8 days after induction (Fig. 4*A*, *left panel*). The *Panx3* mRNA levels in the Panx3-transfected cells were ~100-fold higher than those in the control pEF1-ATDC5 cells at day 8 of induction. At day 16, after induction, the expression of both *Agc1* and *Col10a1* in Panx3-transfected cells was still higher than that of the control cells (Fig. 4*A*). *Panx3* mRNA in the transfected cells at day 16 was increased by about 2-fold, when its level was normalized with the level of control pEF1-transfected cells. The large decrease in the relative ratio of *Panx3* mRNA levels at day 16 compared with day 8 is due to the endogenous *Panx3* mRNA levels increasing substantially from day 8 to 16 as shown in Fig. 2*A*. The actual *Panx3* mRNA levels did not decrease in Panx3-transfected ATDC5 cells during differentiation. Alcian blue staining, often used to stain proteoglycans in cartilage, was also increased in nodules of Panx3-transfected cells compared with the control cells (Fig. 4*B*). We also examined the expression of chondrogenic marker genes in transiently Panx3-transfected N1511 cells during differentiation in the presence of insulin and BMP-2 (Fig. 4*C*). At day 3, the expression of *Col2a1* and *Agc1*

mRNA was stimulated in the transfected cells compared with the control pEF1-transfected cells, whereas the *Col10a1* mRNA levels were very low in both control pEF1- and Panx3-transfected cells. In day 4, *Col10a1* mRNA was induced in control cells, and its expression levels were promoted in Panx3-transfected cells. The total *Panx3* mRNA levels, including exogenous and endogenous *Panx3* mRNA, did not change at day 3 or 4. Taken together, these results indicate that Panx3 expression promoted chondrogenic cell differentiation.

Suppression of Endogenous Panx3 Expression Inhibits Cell Differentiation—To analyze the endogenous Panx3 function in ATDC5 cell differentiation, we knocked down Panx3 expression using Panx3 shRNA. We transfected the Panx3 shRNA expression vector into ATDC5 cells. The resulting stably transfected cells were pooled and induced to differentiate in the presence of insulin. After 8 days in culture, the expression of Panx3 was substantially reduced at both the RNA and protein levels, compared with empty vector-transfected cells (Fig. 5*A*). *Panx3* mRNA was found to be down-regulated by ~70% in Panx3 shRNA-transfected cells compared with the controls. In addition, the expression of mRNA for *Col2a1*, *Agc1*, and *Col10a1* in the shRNA-transfected cells was reduced by 50, 64, and 15%, respectively (Fig. 5*B*). Similarly, Alcian blue staining was reduced to 40% of the control cell level at 16 days in culture (Fig. 5*C*). Similarly, N1511 cell differentiation was inhibited by Panx3 shRNA transfection (data not shown).

To eliminate the possibility of off-target inhibitory effects of shPanx3 on cell differentiation, we used two different types of siRNA for Panx3. Both Panx3 siRNA-1 and -2 inhibited the expression of *Col2a1* and *Col10a1* in ATDC5 cells (Fig. 5*D*). We also tested these siRNAs in primary chondrocytes prepared from cartilage of neonatal mice. Panx3 siRNA-1 and -2 inhibited the expression of *Col10a1* but not *Col2a1* (Fig. 5*E*). This may be because primary chondrocytes are a mixture of different chondrocytes in varying stages of differentiation. The suppression of endogenous Panx3 did not affect *Col2a*-expressing chondrocytes but inhibited differentiation to hypertrophic *Col10a1*-expressing chondrocytes. These results indicate that the suppression of endogenous Panx3 expression inhibited chondrocyte differentiation.

Panx3 Inhibits PTH-induced Cell Proliferation—It has been reported that the expression of connexins such as Cx43, Cx32, and Cx26 inhibits tumor cell growth (27, 28). Panx3 may have similar cell growth inhibitory activity, thereby promoting ATDC5 cell differentiation. Because PTH/PTHrP promotes chondrocyte proliferation, we examined Panx3 activity in PTH-mediated ATDC5 cell proliferation. Three days after the addition of PTH, we found that the number of control ATDC5 cells had increased in a dose-responsive manner and that the maximum cell number was reached at 10 nM PTH (Fig. 6). However, the number of Panx3-transfected ATDC5 cells was reduced in response to increasing amounts of PTH compared with the control cells (Fig. 6*A*). The endogenous PTHrP mRNA levels remained the same in Panx3- and control pEF1-transfected ATDC5 cells, under either proliferation or differentiation conditions (supplemental Fig. 1). PTH/PTHrP receptor was induced during differentiation, but its expression levels were similar in pEF- and Panx3-transfected cells (supplemental Fig. 1). These results suggest that endogenous PTH/PTHrP receptor and PTHrP did not affect the proliferation and differentiation results. This reduced proliferation activity in Panx3-transfected cells with PTH was blocked by anti-Panx3 antibody but not control IgG (Fig. 6*B*). These results suggest that Panx3 inhibits PTH-mediated cell proliferation.

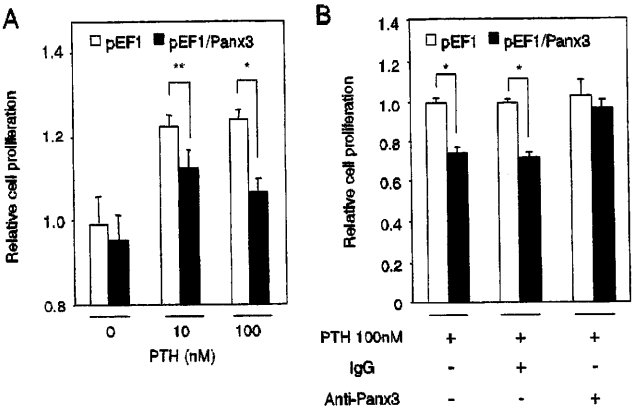

FIGURE 6. **Inhibition of PTH-promoted cell proliferation by Panx3.** *A*, Panx3- and pEF1-transfected cells were incubated in the presence of various amounts of PTH. Cell numbers were counted after 3 days of culture. The number of Panx3-transfected cells was reduced compared with the control cells. *B*, Panx3 antibody, but not IgG, restored PTH-promoted cell proliferation in Panx3-transfected cells. Statistical analysis was performed using analysis of variance (**, $p < 0.02$; *, $p < 0.01$).

Panx3 Reduces Intracellular cAMP and ATP Levels—Because PTH/PTHrP stimulates the proliferation of chondrocytes through activation of the cAMP pathway (2), we examined the intracellular level of cAMP in Panx3-transfected ATDC5 cells under proliferation conditions (Fig. 7*A*). In the absence of PTH, the intracellular cAMP level was ~10% less in Panx3-transfected cells than in control pEF1-transfected cells. The addition of PTH increased the cAMP level within 10 min by 1.7-fold in pEF1-transfected cells. In contrast, Panx3-transfected cells demonstrated only a 1.2-fold induction by PTH. This reduced induction of the cAMP levels in Panx3-transfected cells was reversed to normal levels by addition of anti-Panx3 antibody but not by control IgG (Fig. 7*A*). These data suggest that Panx3 inhibited PTH-mediated proliferation of ATDC5 cells by reducing intracellular cAMP levels.

This result may be due to Panx3 functioning as a hemichannel, releasing ATP to the extracellular space, and thus decreasing the intracellular cAMP level. To examine the hemichannel activity of Panx3, pEF1- and Panx3-transfected ATDC5 cells were treated with PTH, and the release of ATP into the culture medium was then measured (Fig. 7*B*). Panx3-transfected cells exhibited an elevated ATP release that reached a maximum level at 2 min and then gradually decreased with time. A similar release was not observed in control pEF1-transfected cells. In the presence of a high concentration of potassium glutamate (KGlu), which depolarizes the cell membrane, ATP was released from Panx3-transfected ATDC5 cells (Fig. 7*B*). A function-blocking antibody specific to the extracellular domain of Panx3 inhibited this ATP efflux (Fig. 7*C*). This antibody inhibition was blocked by the Panx3 peptide, which was used to raise the Panx3 antibody as an antigen in a dose-dependent manner, whereas its scrambled peptide and control IgG did not affect

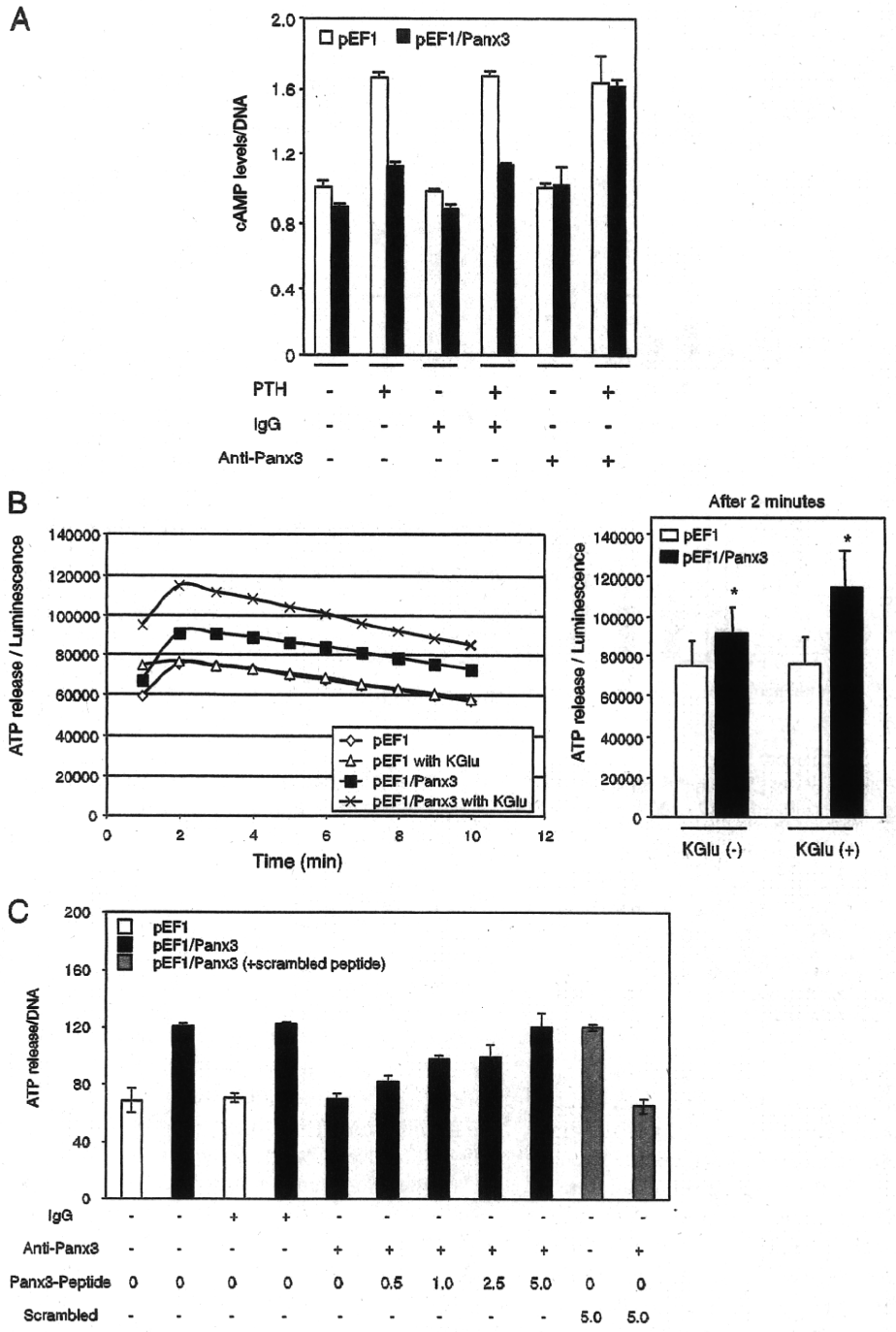

FIGURE 7. **Reduced cAMP levels and increased ATP efflux in Panx3-transfected ATDC5 cells.** *A*, intracellular cAMP level. Panx3- and pEF1-transfected ATDC5 cells were cultured with 10 μg/ml insulin for 1 week. The cells were incubated with anti-Panx3, IgG, or without them for 30 min and then exposed to PTH at 100 nM for 10 min, and we analyzed the intracellular cAMP levels. PTH promoted the intracellular cAMP level in control pEF1-transfected cells, whereas this PTH effect was reduced in Panx3-transfected cells. This reduction was blocked by anti-Panx3 antibody but not IgG. *B*, release of ATP. Cells were plated at ~50% confluency in the absence or presence of potassium (*KGlu*), and ATP levels in the media were measured. ATP release to the extracellular space was increased in Panx3-transfected cells. *Left panel*, time course of ATP release after addition of KGlu. *Right panel*, data at 2 min after addition of KGlu in the *right panel* are shown in *bar graphs*. Statistical analysis was performed using analysis of variance (*, $p < 0.01$). *C*, inhibition of ATP release by Panx3 antibody. Cells were incubated with anti-Panx3 antibody, Panx3 peptide, or IgG for 30 min, and ATP release was measured. The Panx3 antibody inhibited ATP release in Panx3-transfected cells. This inhibition was blocked by various concentrations (0.5 to 5.0 ng/ml) of the Panx3 peptide but not its scrambled peptide (5.0 ng/ml).

the antibody inhibition. These results suggest that the Panx3 hemichannel is one of the major ATP release channels.

Panx3 Inhibits PTH-induced CREB Phosphorylation—We next examined the activation of CREB, which is a downstream molecule of the PTH/PTHrP-cAMP-PKA pathway in chondrocytes (10, 29). CREB reached its maximum phosphorylation level at 30 min after PTH treatment in the control pEF1-transfected ATDC5 cells. In Panx3-transfected cells, CREB phosphorylation was significantly reduced (Fig. 8*A*). The reduced CREB phosphorylation in Panx3-transfected cells was blocked by anti-Panx3 antibody but not by IgG (Fig. 8*B*). Taken together, these results suggest that Panx3 inhibits PTH/PTHrP-cAMP-PKA signaling in ATDC5 cells.

DISCUSSION

In this study, we utilized a bioinformatics approach to search for a gap junction protein involved in cartilage development. We found that *Panx3* mRNA was preferentially expressed in a transitional stage between proliferative chondrocytes and terminally differentiated hypertrophic chondrocytes in developing growth plates. This suggests that Panx3 plays a role in the switch from proliferation to differentiation in these chondrocytes. To assess Panx3 action in chondrocyte differentiation, we used chondrogenic cell lines ATDC5 and N1511, which can be induced to differentiate into chondrocyte phenotypes. *Panx3* mRNA expression was induced during differentiation of ATDC5 and N1511 cells (Fig. 2). We demonstrated that the expression of Panx3 promoted differentiation of ATDC5 and N1511 cells (Fig. 4). In contrast, the inhibition of endogenous Panx3 expression through Panx3 shRNA and siRNA reduced differentiation of these cells and primary chondrocytes (Fig. 5 and data not shown) These results suggest that Panx3 regulates chondrogenic cell differentiation.

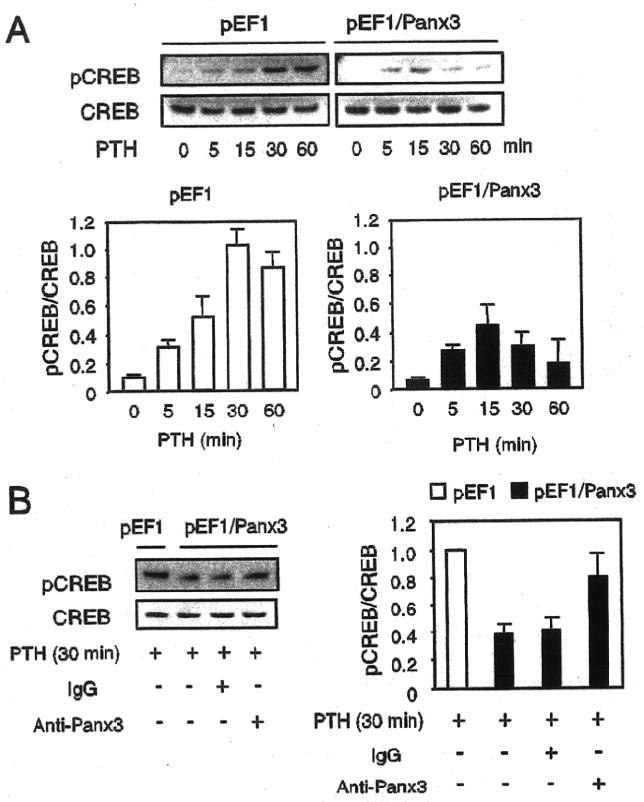

FIGURE 8. **Decrease in phosphorylation of CREB by Panx3.** *A*, time course of CREB phosphorylation. ATDC5 cells were cultured with 10 μg/ml insulin for 1 week and then treated with PTH (100 nM) for the time indicated. Protein extracts were analyzed by Western blotting using anti-phospho-CREB and anti-CREB antibodies. In control pEF1-transfected cells, the phosphorylation of CREB was strongly induced, and in Panx3-transfected cells the phosphorylation levels of CREB were reduced. *B*, restoration of the CREB phosphorylation levels by Panx3 antibody. Cells were preincubated with Panx3 antibody or IgG for 30 min before the stimulation with 100 nM PTH, and then Western blotting using anti-phospho-CREB and anti-CREB antibodies was performed. Panx3 antibody inhibited the reduction of the phosphorylation of CREB in Panx3-transfected cells. ImageJ 1.33u was used to quantify the protein bands.

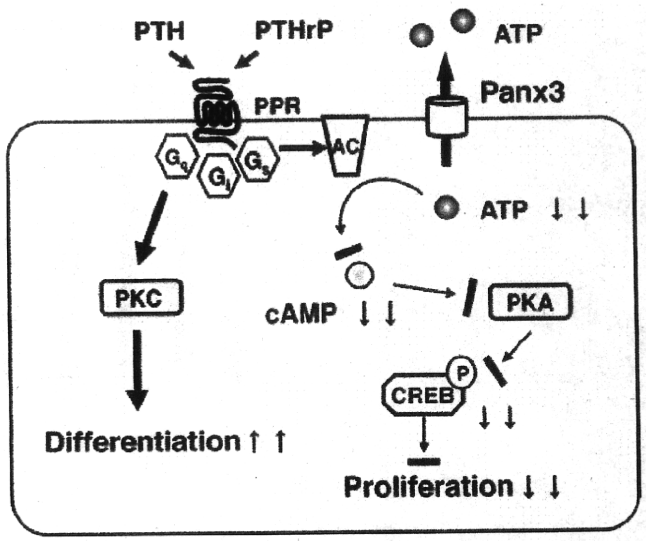

FIGURE 9. **Role of Panx3 in chondrogenic differentiation.** The PTH/PTHrP receptor activates multimeric G proteins. The activation of the G_s subunit leads to the activation of adenylyl cyclase (*AC*) for cAMP generation from ATP and the subsequent activation of PKA. PKA phosphorylates CREB, which promotes the expression of genes for cell proliferation. Panx3 is expressed in prehypertrophic chondrocytes, and it promotes the release of ATP into the extracellular space, which results in a reduction of the intracellular cAMP level and subsequent inhibition of PKA/CREB signaling for cell proliferation. The PTH/PTHrP receptor also activates the G_q subunit and subsequent downstream signaling, such as protein kinase C (*PKC*), to promote differentiation.

PTH/PTHrP functions to keep chondrocytes proliferating and to delay hypertrophic chondrocyte differentiation. Both PTHrP-deficient mice and PTH/PTHrP receptor-deficient mice have similar growth plate abnormalities, *i.e.* reduced numbers of chondrocytes and premature hypertrophic differentiation, indicating that PTHrP signals primarily through the PTH/PTHrP receptor in the growth plate (3, 5). We found that PTH increased proliferation of ATDC5 cells in culture, but this PTH activity was reduced in Panx3-transfected ATDC5 cells (Fig. 6). There was no significant difference in cell proliferation activity between untransfected and Panx3-transfected ATDC5 cells in the absence of PTH, indicating that the inhibitory activity of Panx3 for cell proliferation is dependent on PTH. The interaction of PTH/PTHrP with PTH/PTHrP receptor promotes the activation of multiple heteromeric G proteins, including G_s, which can activate adenylyl cyclase, G_q, which can activate phospholipase C/protein kinase C, and G_q, whose action occurs opposite the G_s pathway (30, 31). The PTH-induced activation of G_s leads to the cascade activation of downstream molecules, specifically the activation of adenylyl cyclase, an increase in cAMP levels, the activation of PKA, and the phosphorylation of CREB. The activation of CREB induces the expression of genes required for cell proliferation (Fig. 9).

We found that Panx3 expression in ATDC5 cells promoted ATP release from the cytoplasm to the extracellular space, and this ATP release was inhibited by a function-blocking anti-Panx3 antibody, suggesting that Panx3 plays a specific role in the release of ATP (Fig. 7, *B* and *C*). The activity of Panx3 as a hemichannel for ATP release would explain the reduced intracellular cAMP levels in Panx3-expressing ATDC5 cells treated with PTH, because ATP is converted to cAMP by adenylyl cyclase (32). Thus, it is conceivable that Panx3-promoted ATP release to the extracellular space results in the reduction of intracellular cAMP, leading to the inhibition of PTH-induced cell proliferation. Panx3 activity in ATDC5 cells as an ATP-release channel is consistent with recent reports that Panx1 can form a hemichannel for stress-sensitive ATP permeability in oocytes and erythrocytes (19, 33).

ATP secreted into the pericellular environment affects a variety of cellular processes. Recently, up-regulation of Panx1 has been reported in macrophages stimulated by endotoxin lipopolysaccharide. This treatment mediates large pore formation of the ATP-gated $P2X_7Rs$ receptor, which leads to interleukin-1 release from the activated macrophage (34). The interaction of ATP with P2 receptors reportedly increases the concentration of intracellular Ca^{2+} in chondrocytes through G_q (35). ATP released into the extracellular space through Panx3 hemichannels at the early differentiation stage may re-enter the cytoplasm through purinergic receptors such as P2Y and P2X and promote differentiation. It is also possible that Panx3 may function as a Ca^{2+} channel in the ER and increase intracellular Ca^{2+} levels for chondrocyte maturation.

Although Panx3 mRNA is expressed strongly by prehypertrophic chondrocytes, the Panx3 protein is found in both prehypertrophic and hypertrophic chondrocytes (Fig. 1). We did not detect Panx1 or Panx2 in developing growth plates with *in situ* hybridization (data not shown). Panx1, but not Panx2, was expressed very weakly in ATDC5 cells but was not induced during ATDC5 cell differentiation (data not shown). Connexin43 is expressed in condensing mesenchymal cells in the primordial cartilage, and also in articular chondrocytes and osteoblasts. Connexin43 has been shown to form functional gap junctions capable of sustaining the propagation of intercellular Ca^{2+} waves in articular chondrocyte culture (36) and to regulate BMP-2-mediated chondrogenic differentiation in chick mesenchyme micromass culture (37). Many mutations in the connexin43 gene have been identified in association with oculodentodigital dysplasia (38, 39), which is characterized by syndactyly of the hands and feet, hypoplasia of the middle phalanges, and abnormal craniofacial elements. However, connexin-deficient mice do not exhibit any of the gross abnormalities of chondrocyte differentiation, but they do have mineralization defects (40). Immunostaining of developing growth plates revealed that connexin43 was not expressed in prehypertrophic and hypertrophic chondrocytes, but it was expressed in osteoblasts (data not shown). These connexin43 expression patterns are consistent with the skeletal phenotype of connexin43-deficient mice. Thus, Panx3 is likely the major gap junction protein in cartilage.

In conclusion, we demonstrated that Panx3 is uniquely expressed in prehypertrophic and hypertrophic chondrocytes and that it promotes the chondrogenic differentiation of ATDC5 cells, at least in part through its hemichannel activity. Panx3 inhibits PTH-induced ATDC5 cell proliferation and mediates intracellular ATP release into the extracellular space, which in turn leads to a reduction in cAMP/PKA signaling, resulting in decreased proliferation and increased differentiation. Our findings suggest that Panx3 is a regulator of the switching mechanism behind the transition of chondrocytes from a proliferative state to a postmitotic state and that it is required for chondrocyte differentiation.

Acknowledgments—We thank Dr. Masahiro Iwamoto for plasmid Hist1h4c and Dr. Motomi Iwamoto and Dr. Hideto Watanabe for N1511 cells.

REFERENCES

1. Kronenberg, H. M. (2003) *Nature* **423,** 332–336
2. Kronenberg, H. M. (2006) *Ann. N.Y. Acad. Sci.* **1068,** 1–13
3. Karaplis, A. C., Luz, A., Glowacki, J., Bronson, R. T., Tybulewicz, V. L., Kronenberg, H. M., and Mulligan, R. C. (1994) *Genes Dev.* **8,** 277–289
4. Miao, D., He, B., Karaplis, A. C., and Goltzman, D. (2002) *J. Clin. Invest.* **109,** 1173–1182
5. Lanske, B., Karaplis, A. C., Lee, K., Luz, A., Vortkamp, A., Pirro, A., Karperien, M., Defize, L. H., Ho, C., Mulligan, R. C., Abou-Samra, A. B., Jüppner, H., Segre, G. V., and Kronenberg, H. M. (1996) *Science* **273,** 663–666
6. Weir, E. C., Philbrick, W. M., Amling, M., Neff, L. A., Baron, R., and Broadus, A. E. (1996) *Proc. Natl. Acad. Sci. U.S.A.* **93,** 10240–10245
7. Schipani, E., Lanske, B., Hunzelman, J., Luz, A., Kovacs, C. S., Lee, K., Pirro, A., Kronenberg, H. M., and Jüppner, H. (1997) *Proc. Natl. Acad. Sci. U.S.A.* **94,** 13689–13694
8. Abou-Samra, A. B., Jüppner, H., Force, T., Freeman, M. W., Kong, X. F., Schipani, E., Urena, P., Richards, J., Bonventre, J. V., and Potts, J. T., Jr. (1992) *Proc. Natl. Acad. Sci. U.S.A.* **89,** 2732–2736
9. Singh, A. T., Gilchrist, A., Voyno-Yasenetskaya, T., Radeff-Huang, J. M., and Stern, P. H. (2005) *Endocrinology* **146,** 2171–2175
10. Beier, F., Ali, Z., Mok, D., Taylor, A. C., Leask, T., Albanese, C., Pestell, R. G., and LuValle, P. (2001) *Mol. Biol. Cell* **12,** 3852–3863
11. Beier, F., and LuValle, P. (2002) *Mol. Endocrinol.* **16,** 2163–2173
12. Panchin, Y., Kelmanson, I., Matz, M., Lukyanov, K., Usman, N., and Lukyanov, S. (2000) *Curr. Biol.* **10,** R473–R474
13. Baranova, A., Ivanov, D., Petrash, N., Pestova, A., Skoblov, M., Kelmanson, I., Shagin, D., Nazarenko, S., Geraymovych, E., Litvin, O., Tiunova, A., Born, T. L., Usman, N., Staroverov, D., Lukyanov, S., and Panchin, Y. (2004) *Genomics* **83,** 706–716
14. Vogt, A., Hormuzdi, S. G., and Monyer, H. (2005) *Brain Res. Mol. Brain Res.* **141,** 113–120
15. Penuela, S., Bhalla, R., Gong, X. Q., Cowan, K. N., Celetti, S. J., Cowan, B. J., Bai, D., Shao, Q., and Laird, D. W. (2007) *J. Cell Sci.* **120,** 3772–3783
16. Penuela, S., Celetti, S. J., Bhalla, R., Shao, Q., and Laird, D. W. (2008) *Cell Commun. Adhes.* **15,** 133–142
17. Wang, X. H., Streeter, M., Liu, Y. P., and Zhao, H. B. (2009) *J. Comp. Neurol.* **512,** 336–346
18. Bruzzone, R., Hormuzdi, S. G., Barbe, M. T., Herb, A., and Monyer, H. (2003) *Proc. Natl. Acad. Sci. U.S.A.* **100,** 13644–13649
19. Bao, L., Locovei, S., and Dahl, G. (2004) *FEBS Lett.* **572,** 65–68
20. Vanden Abeele, F., Bidaux, G., Gordienko, D., Beck, B., Panchin, Y. V., Baranova, A. V., Ivanov, D. V., Skryma, R., and Prevarskaya, N. (2006) *J. Cell Biol.* **174,** 535–546
21. Atsumi, T., Miwa, Y., Kimata, K., and Ikawa, Y. (1990) *Cell Differ. Dev.* **30,** 109–116
22. Kamiya, N., Jikko, A., Kimata, K., Damsky, C., Shimizu, K., and Watanabe, H. (2002) *J. Bone Miner. Res.* **17,** 1832–1842
23. Williams, J. A., Kondo, N., Okabe, T., Takeshita, N., Pilchak, D. M., Koyama, E., Ochiai, T., Iensen, D., Chu, M. L., Kane, M. A., Napoli, J. L., Enomoto-Iwamoto, M., Ghyselinck, N., Chambon, P., Pacifici, M., and Iwamoto, M. (2009) *Dev. Biol.* **328,** 315–327
24. Shukunami, C., Ohta, Y., Sakuda, M., and Hiraki, Y. (1998) *Exp. Cell Res.* **241,** 1–11
25. Nakamura, K., Shirai, T., Morishita, S., Uchida, S., Saeki-Miura, K., and Makishima, F. (1999) *Exp. Cell Res.* **250,** 351–363
26. Watanabe, H., de Caestecker, M. P., and Yamada, Y. (2001) *J. Biol. Chem.* **276,** 14466–14473
27. Kumar, N. M., and Gilula, N. B. (1996) *Cell* **84,** 381–388
28. Yamasaki, H., and Naus, C. C. (1996) *Carcinogenesis* **17,** 1199–1213
29. Ionescu, A. M., Schwarz, E. M., Vinson, C., Puzas, J. E., Rosier, R., Reynolds, P. R., and O'Keefe, R. J. (2001) *J. Biol. Chem.* **276,** 11639–11647
30. Bringhurst, F. R., Juppner, H., Guo, J., Urena, P., Potts, J. T., Jr., Kronenberg, H. M., Abou-Samra, A. B., and Segre, G. V. (1993) *Endocrinology* **132,** 2090–2098
31. Schwindinger, W. F., Fredericks, J., Watkins, L., Robinson, H., Bathon, J. M., Pines, M., Suva, L. J., and Levine, M. A. (1998) *Endocrine* **8,** 201–209
32. Cooper, D. M. (2003) *Biochem. J.* **375,** 517–529
33. Locovei, S., Wang, J., and Dahl, G. (2006) *FEBS Lett.* **580,** 239–244
34. Pelegrin, P., and Surprenant, A. (2006) *EMBO J.* **25,** 5071–5082
35. Kaplan, A. D., Kilkenny, D. M., Hill, D. J., and Dixon, S. J. (1996) *Endocrinology* **137,** 4757–4766
36. Tonon, R., and D'Andrea, P. (2000) *J. Bone Miner. Res.* **15,** 1669–1677
37. Zhang, W., Green, C., and Stott, N. S. (2002) *J. Cell. Physiol.* **193,** 233–243
38. Richardson, R., Donnai, D., Meire, F., and Dixon, M. J. (2004) *J. Med. Genet.* **41,** 60–67
39. Kjaer, K. W., Hansen, L., Eiberg, H., Leicht, P., Opitz, J. M., and Tommerup, N. (2004) *Am. J. Med. Genet.* **127A,** 152–157
40. Lecanda, F., Warlow, P. M., Sheikh, S., Furlan, F., Steinberg, T. H., and Civitelli, R. (2000) *J. Cell Biol.* **151,** 931–944

ARCHIVES OF ORAL BIOLOGY 55 (2010) 426–434

available at www.sciencedirect.com

ScienceDirect

journal homepage: http://www.elsevier.com/locate/aob

PDGFs regulate tooth germ proliferation and ameloblast differentiation

Nan Wu [a,c], Tsutomu Iwamoto [b,*], Yu Sugawara [b], Masaharu Futaki [b], Keigo Yoshizaki [a], Shinya Yamamoto [a], Aya Yamada [b], Takashi Nakamura [b], Kazuaki Nonaka [a], Satoshi Fukumoto [b,*]

[a] Section of Pediatric Dentistry, Division of Oral Health, Growth and Development, Faculty of Dental Science, Kyushu University, Fukuoka 812-8582, Japan

[b] Division of Pediatric Dentistry, Department of Oral Health and Development Sciences, Tohoku University Graduate School of Dentistry, Sendai 980-8575, Japan

[c] Department of Pediatric Dentistry, Peking University School and Hospital of Stomatology, Beijing 100081, PR China

ARTICLE INFO

Article history:
Accepted 12 March 2010

Keywords:
Tooth development
PDGF
Organ culture
Cusp
Ameloblastin

ABSTRACT

Objective: The purpose of this study was to elucidate the effects of platelet-derived growth factors (PDGFs) during tooth development, as well as the mechanisms underlying the interactions of growth factors with PDGF signalling during odontogenesis.

Design: We used an *ex vivo* tooth germ organ culture system and two dental cell lines, SF2 cells and mDP cells, as models of odontogenesis. AG17, a tyrosine kinase inhibitor, was utilised for blocking PDGF receptor signalling. To analyse the expressions of PDGFs, reverse transcriptase (RT)-PCR and immunohistochemistry were performed. Proliferation was examined using a BrdU incorporation assay for the organ cultures and a cell counting kit for the cell lines. The expressions of Fgf2 and ameloblastin were analysed by real-time RT-PCR.

Results: The PDGF ligands PDGF-A and PDGF-B, and their receptors, PDGFRα and PDGFRβ, were expressed throughout the initial stages of tooth development. In the tooth germ organ cultures, PDGF-AA, but not PDGF-BB, accelerated cusp formation. Conversely, AG17 suppressed both growth and cusp formation of tooth germs. Exogenous PDGF-BB promoted mDP cell proliferation. Furthermore, PDGF-AA decreased Fgf2 expression and increased that of ameloblastin, a marker of differentiated ameloblasts.

Conclusion: Our results indicate that PDGFs are involved in initial tooth development and regulate tooth size and shape, as well as ameloblast differentiation.

1. Introduction

The process of tooth development depends on well-regulated reciprocal epithelial–mesenchymal interactions that are mediated by multiple signalling pathways.[1] Mouse molar tooth development is initiated as a thickening of oral epithelium to form a dental placode, which subsequently continues to grow and invaginate into the

* *Corresponding authors.* Fax: +81 22 717 8386.
E-mail addresses: tiwamoto@m.tains.tohoku.ac.jp (T. Iwamoto), fukumoto@mail.tains.tohoku.ac.jp (S. Fukumoto).

0003–9969/$ – see front matter
doi:10.1016/j.archoralbio.2010.03.011

underlying dental mesenchyme derived from cranial neural crest cells. Consequently, differential cell proliferation in the dental epithelium results in the formation of tooth cusps, which pre-pattern the final shape of each individual tooth. Finally, dental epithelial cells differentiate into ameloblasts, which secrete enamel specific matrix proteins, including amelogenin, ameloblastin and enamelin.

Platelet-derived growth factors (PDGFs) bind strongly to their receptors and are thought to play important roles in epithelial–mesenchymal interactions to regulate cell proliferation, migration, extracellular matrix synthesis and deposition in organogenesis.[2] PDGFs consist of four member ligands, PDGF-A, -B, -C and -D, which compose disulphide-linked homodimers, except for PDGF-AB, and act via two different receptor tyrosine kinases, PDGFRα and β. Homodimers of PDGFRα bind PDGF-A, -B and -C, while those of PDGFRβ bind PDGF-B and -D.[3]

PDGF ligands and their receptors are expressed during critical phases of mouse embryogenesis, and play important roles in multiple organ development including tooth.[4–11] PDGF-A null-mice die either as embryos or shortly after birth due to lung emphysema.[4,5] PDGFRα deficient mice also die during embryonic development, and exhibit incomplete cephalic closure.[6,7] In addition, PDGF-B and PDGFRβ knockout mice die during late gestation, due to cardiovascular complications caused by the absence of vascular smooth muscle cells and/or pericytes, and the lack of mesangial cells of the kidney glomerulus suggest the failure of mesenchymal progenitors to locate to their appropriate final destination.[8–11] Our previous work demonstrated that knockdown of PDGF-AA and -BB gene by siRNA dramatically inhibited salivary gland branching morphogenesis, indicated that PDGF signalling is involved in salivary gland morphogenesis, and PDGFs modulate Fgfs expressions through the interaction between epithelial and neural crest-derived mesenchyme.[12] In tooth development, PDGFRα null mutant mice showed inhibition of cusp formation by tooth germs.[13] Transplantation of tooth germ of PDGFRα null mutant mice into a kidney capsule revealed that it does not affect proper odontoblasts proliferation and differentiation in the cranial neural crest-derived odontogenic mesenchyme but perturbs the formation of extracellular matrix and the organisation of odontoblast cells at the forming cusp area, resulting in dental cusp growth defect.[13] However, during tooth morphogenesis, the effects of PDGFs on tooth development and mechanisms of the underlying growth factors that interact with PDGF signalling have not been clearly elucidated.

In the present study, we examined the role of PDGF signalling in tooth development using tooth germ organ culture systems. We found that PDGF-AA accelerated cusp formation, whereas PDGF-BB did not. Furthermore, treatment with AG17, a tyrosine kinase inhibitor, suppressed growth and cusp formation of tooth germs. We also noted that PDGF-AA decreases Fgf2 expression and increases that of ameloblastin. Together, our results indicate that PDGFs regulate tooth size and shape, as well as the differentiation of ameloblasts.

2. Materials and methods

2.1. *Animal and tissue preparations*

Pregnant ICR mice were provided by Japan SLC, Inc. The presence of a vaginal plug was used as an indication of pregnancy day 0 (E0). The first mandibular molar tooth germs were dissected under stereomicroscope and used for organ cultures. The dental epithelia and mesenchymal tissue samples were separated by treatment with dispase, as reported previously.[12]

2.2. *Immunostaining*

ICR mouse embryo heads were dissected and embedded in OCT compound (Sakura Finetechnical Co.) for frozen sectioning. OCT blocks were cut into 8-μm sections with a cryostat (2800 FRIGOCUT, Leica), held for 30 min at room temperature and then fixed in 4% PFA for 5 min. After washing 3 times with PBS for 5 min each, liberate antibody binding solution (LAB, Polysciences, Inc.) was applied for 5 min for activation of the binding sites, then washing with PBS was performed. Blocking with Power Block (BioGenex) was performed for 5 min, then the specimens were incubated with the primary antibody for 1 h. After washing 3 times with TPBS for 10 min each, the specimens were incubated with the secondary antibody for 30 min, followed by another washing with TPBS. Finally, the sections were mounted with Vectashield (Vector Labs). A fluorescent microscope (Biozero-8000, Keyence, Japan) was utilised for immunostaining image analysis. The antibodies used were previously described.[12]

2.3. *Semiquantitative and real-time* RT-PCR

Total RNA was isolated using TRIzol reagent (Invitrogen) according to the manufacturer's protocol. First strand cDNA was synthesised at 42 °C for 90 min using oligo(dT)$_{14}$ primer with SuperScript III (Invitrogen). PCR amplification was performed using Taq DNA polymerase (TAKARA, Japan), with the PCR products separated on a 1.5% agarose gel. Real-time RT-PCR was carried out with SYBR Green PCR Master Mix. A TaqMan 7700 Sequencer (Applied Biosystems) was used for the amplification process. PCR was performed for 40 cycles at 95 °C for 1 min and 60 °C for 1 min, and 72 °C for 1 min. The primer sequences used for PDGF-A were 5′-caagaccaggacggtcattt-3′ and 5′-cctcacctggacctct-ttca-3′ (223), while those for PDGF-B were 5′-gcagggtgag-caaggttgtaatg-3′ and 5′-tgaaggaagcagaaggaacgg-3′ (514), for PDGFRα were 5′-acagagactgagcgctgaca-3′ and 5′-caccag-gtccgaggaatcta-3′(226), for PDGFRβ were 5′-acgtaccctacgac-caccag-3′ and 5′-tccattggaagttcaccaca-3′ (234), for Bmp4 were 5′-actgccgcagcttctctgag-3′ and 5′-ttctccagatgttcttcgtg-3′ (485), for CK14 were 5′-tgggtggagatgtcaatgtg-3′ and 5′-ctgccaatcatctcctggat-3′ (446), for HPRT were 5′-gcgtcgt-gattagcgatgatga-3′ and 5′-gtcaagggcatatccaacaaca-3′ (563), for Fgf2 5′-gcgagaagagcgacccacac-3′ and 5′-gaagccag-cagccgtccatc-3′ (124), for ameloblastin 5′-ttgaatgctcctgcca-gaatcg-3′ and 5′-taagggtttgcctgaagcctcc-3′ (118) and for glyceraldehyde-3-phosphate dehydrogenase (GAPDH) were

5′-ggagcgagacccctctaacatc-3′ and 5′-ctcctggttcacacccatcac-3′ (181).

2.4. *Ex vivo tooth germ organ culture*

Mandibular first molar germs from E13.5/E14.5 ICR mouse embryos were dissected using chemically defined medium in a modification of Trowell's system[14] and cultured on cell culture inserts (353090 BD Falcon) at the air/medium interface. Two tooth germs from each mandible were divided into the control and experimental groups. The inserts were floated on 2 ml of BGjb media in 6-well compartments of TC Plates (353502 BD Falcon). To the BGJb we added 0.5%/10% FBS, 100 U/ml of penicillin–streptomycin and 100 μg/ml of ascorbic acid. Ten of the tooth germs were cultured in humidified 5% CO_2/95% air. PDGF-AA (lot 24087, UPSTATE) or PDGF-BB (lot ZT02, SYSTEMS) was added to the media as exogenous PDGF. AG17, a selective inhibitor of the PDGF receptor tyrosine kinase, was used to arrest the function of PDGFRα and PDGFRβ. The tooth germs were photographed every day and tooth size was measured using a computer to evaluate their growth. Each experiment was repeated 3 times.

2.5. *BrdUrd incorporation assay*

Tooth germs were cultured with or without AG17 for 5 days, then stained with a 5-Bromo-2′-deoxy-uridine Labeling and Detection Kit I (Roche) according to the manufacturer's protocol. Briefly, BrdUrd was added to the plates (10 mm) for 1 h, and washed with PBS. Then the tooth germs were embedded into paraffin. Paraffin sections from the embedded organ were generated and placed on glass slides. The specimens were dewaxed. After washing 3 times in PBS, the organs were incubated for 30 min with a 1:50 dilution of fluorescein isothiocyanate-conjugated anti-BrdUrd antibody at room temperature. Finally, after washing the organs in PBS 3 times, the nuclei were stained with propidium iodide (Vector Laboratories) and BrdUrd-positive cells were examined under a microscope (Biozero-8000; Keyence, Japan).

2.6. *Dental cell culture and cell proliferation assay*

Two different dental cell lines were used to examine the functions of PDGFs; SF2 cells, from an epithelial cell line, and mDP cells, from a dental mesenchymal cell line. They were maintained in Dulbecco's modified Eagle's medium/F-12 medium supplemented with 10% foetal bovine serum, and 1% penicillin and streptomycin at 37 °C in a humidified atmosphere containing 5% CO_2.[15,16] Cell proliferation was assessed using a Cell counting kit-8 containing WST-8 (2-[2-methoxy-4-nitrophenyl]-3-[4-nitrophenyl]-5-[2,4-disulphophenyl]-2H-tetrazolium, monosodium salt) (Dojindo Laboratories). SF2 and mDP cells were separately inoculated at 4000 cell per/well (96-well plates), then cultured in the presence or absence of 5 ng/ml of PDGF-AA or PDGF-BB recombinant proteins for 1, 3 and 5 days. After a 1-h incubation with WST-8 at 0.5 mM, cell proliferation activity was determined calorimetrically at 450 nm, as described in the manual provided by the manufacturer.

3. Results

3.1. *Expressions of PDGF-A, PDGF-B, PDGFRα and PDGFRβ in developing tooth germs*

First, we examined the mRNA expressions of PDGF-A, PDGF-B, PDGFRα and PDGFRβ during tooth germ development by RT-PCR. All PDGF ligands and their receptors were expressed during the initial stages of tooth germ development (Fig. 1A). Tooth development had reached the cap stage by E14.5, at the time when PDGF-A mRNA was strongly expressed in dental epithelium and weakly expressed in dental mesenchyme, while PDGF-B mRNA was expressed in both dental epithelium and mesenchyme and PDGFRα and PDGFRβ were preferentially expressed in dental mesenchyme, and faintly expressed in dental epithelium (Fig. 1B). Immunostaining with specific antibodies for PDGF-A, PDGF-B, PDGFRα and PDGFRβ revealed their protein expressions during initial tooth development. PDGF-A and -B proteins were strongly associated with dental and oral epithelia, and diffusely distributed throughout the dental mesenchyme (Fig. 1C). PDGFRα and PDGFRβ proteins were mainly expressed in the dental mesenchyme during initial tooth development. In the dental epithelium, PDGFRα protein was observed at the inner enamel epithelium by E15.5 (Fig. 1C). PDGFRβ protein was observed in the enamel knot on E14.5, and was also likely in the stratum intermedium on E16.5 (Fig. 1C). Overall, PDGF ligands and their receptors were expressed throughout the initial stages of tooth development, indicating their involvement in that process.

3.2. *AG17 inhibits tooth germ growth and cusp formation*

To analyse the functional importance of PDGFs in tooth development, we used a tooth molar organ culture system with or without AG17, a tyrosine kinase inhibitor, to determine its inhibition of PDGFRα and PDGFRβ signalling. Under a normal condition, tooth germs from E13.5 mice grew and formed cusp-like structures after 5 days of culture (Fig. 2A). In contrast, in the presence of AG17, tooth germ growth and cusp formation were blocked (Fig. 2A), with tooth germ width, height and cusp height inhibited by 17%, 22% and 40%, respectively (Fig. 2B). These results suggest that PDGF signalling is essential for tooth germ growth and cusp formation.

Next, we investigated the involvement of PDGFRα and PDGFRβ in cell proliferation and cusp formation. Since AG17 blocked tooth germ growth, we examined its effect on cell proliferation. Tooth germs from E13.5 mice were treated with or without AG17 for 5 days, and cell proliferation was analysed by BrdU incorporation after 1 h (Fig. 3A). Inner enamel epithelium (Fig. 3A) and dental papilla facing dental epithelium (Fig. 3A) had a large number of BrdU-positive cells. On the other hand, the stratum intermedium, stellate reticulum and dental papilla, except for the dental papilla 1 area, showed fewer BrdU-positive cells as compared to the inner enamel epithelium and dental papilla 1 area. Furthermore, the numbers of BrdU-positive cells were decreased in all cells in both dental epithelium and mesenchyme exposed to AG17 (Fig. 3B, C). These results indicate that suppression of PDGFR signalling inhibits cell proliferation in developing tooth germs.

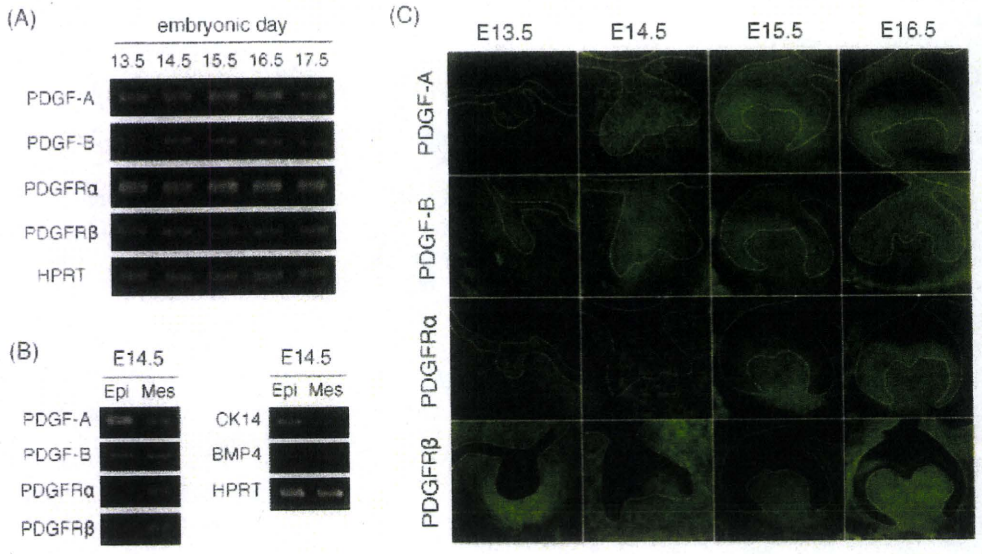

Fig. 1 – Expressions of PDGF-A, PDGF-B, PDGFRα and PDGFRβ in developing tooth germs. (A) The expressions of mRNAs for PDGFs and PDGFRs were analysed in tooth germs from embryonic day (E)13.5 to E17.5 by RT-PCR. PDGFs were expressed in all initial stages of tooth germ development. Hypoxanthine phosphoribosyltransferase (HPRT) gene was used as an internal control. (B) Tooth germs were dissected on E14.5, the cap stage, and dental epithelium (*Epi*) and mesenchyme (*Mes*) were separated under a microscope. RT-PCR revealed that PDGF-A mRNA was strongly expressed in the dental epithelium, PDGF-B mRNA was expressed in both dental epithelium and mesenchyme, and PDGFRα and PDGFRβ were preferentially expressed in dental mesenchyme, and faintly expressed in dental epithelium. Cytokeratin-14 (CK14) and Bmp4 were used as markers for dental epithelium and mesenchyme, respectively. (C) Immunostaining for PDGFs in tooth germ development. PDGF-A and -B were strongly expressed in dental epithelium, while PDGFRα and PDGFRβ proteins were mainly expressed in dental mesenchyme. In dental epithelium, PDGFRα protein was observed from E13.5, though its expression eventually shifted to the inner enamel epithelium by E15.5. PDGFRβ protein was located in the enamel knot on E14.5, after which PDGFRβ protein was present in the stratum intermedium on E16.5. Broken white lines, determined by immunostaining with laminin antibody (data not shown), indicate the basement membrane.

3.3. *PDGF-BB promotes cell proliferation of dental mesenchymal cells*

We also examined the effects of PDGF-AA and -BB on proliferation of the dental epithelial cell line SF2 and dental mesenchyme cell line mDP. Both types of cells were cultured in the presence of PDGF-AA or -BB for 5 days, and cell proliferation was analysed using a cell counting kit. We found that neither had an effect on SF2 proliferation after 5 days (Fig. 4A). In contrast, PDGF-BB promoted mDP cell proliferation, whereas

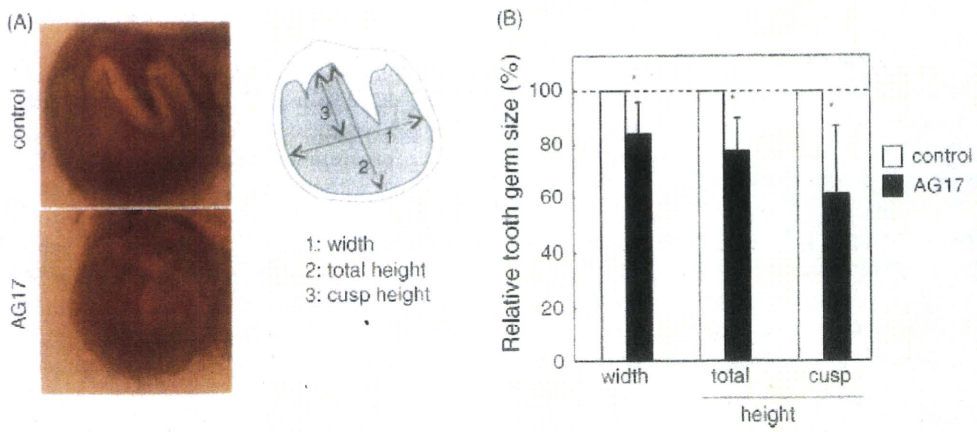

Fig. 2 – AG17 blocks tooth germ growth and cusp formation. (A) Tooth germs obtained on E13.5 were cultured with or without 500 ng/ml of AG17 for 5 days. (B) Tooth germ width, height and cusp height were measured. AG17 was found to inhibit tooth germ growth and cusp formation.

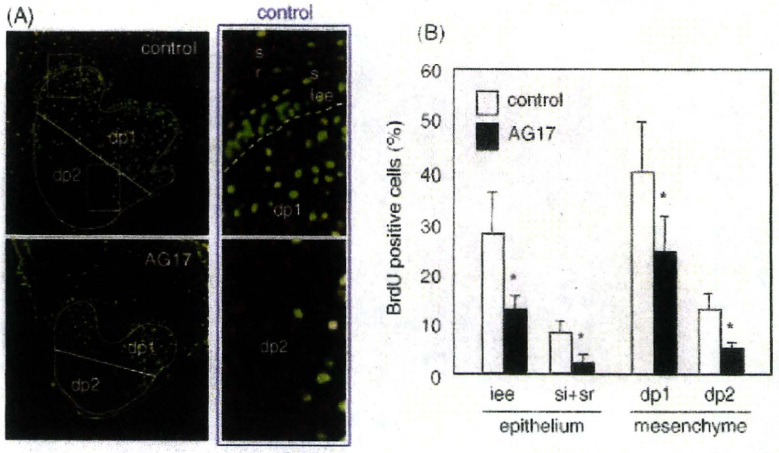

Fig. 3 – AG17 inhibits tooth germ cell proliferation. (A, B) Tooth germs were cultured with or without 500 ng/ml of AG17 for 5 days, then BrdU incorporation after 1 h was analysed using a fluorescence microscope. AG17 inhibited both dental epithelium and mesenchyme cells in the tooth germs. For this experiment, dental papilla sections were divided equally into two parts (DP1 and DP2). Statistical analysis was performed using analysis of variance (*$p < 0.05$). *iee*; inner enamel epithelium, *si*; stratum intermedium, *sr*; stellate reticulum.

PDGF-AA did not (Fig. 4B). On the other hand, AG17 inhibited cell proliferation of both types of cells regardless of PDGF treatment (Fig. 4A, B). These results indicate that PDGF-AA signalling may not take part in cell proliferation in dental epithelial cells, and PDGF-BB signalling is important for dental mesenchymal cell proliferation. Furthermore, results showing that AG17 has an effect on cell proliferation indicate that autocrine effects of PDGF-AA and -BB may be important for proliferation of tooth cells.

3.4. *PDGF-AA accelerates cusp formation*

Analysis of cell proliferation using dental cells showed that PDGF-BB accelerates dental mesenchymal proliferation. However, since the role of PDGF-AA in tooth development remains unclear, we cultured tooth germs taken on E13.5 with PDGF-AA or -BB for 7 days, and analysed dental cusp formation. To evaluate the effects of those PDGFs on cusp formation, we divided tooth development into 4 stages, as follows: the initial stage (S-I), the stage in which the tooth germ grows and becomes round (S-II), the stage in which the initial sign of a tooth cusp can be identified (S-III) and the stage in which the tooth cusp can be clearly identified and becomes sharp (S-IV) (Fig. 5A). When the total percentage of tooth germs classified as S-III and S-IV following treatment with PDGF-AA was compared to non-treated tooth germs, those with PDGF-AA treatment had cusp formation that was greater by 1.5- and 1.2-fold on days 5 and 6, respectively (Fig. 5B). However, there was no difference in cusp formation between tooth germs treated with and without PDGF-BB (data not shown). These findings

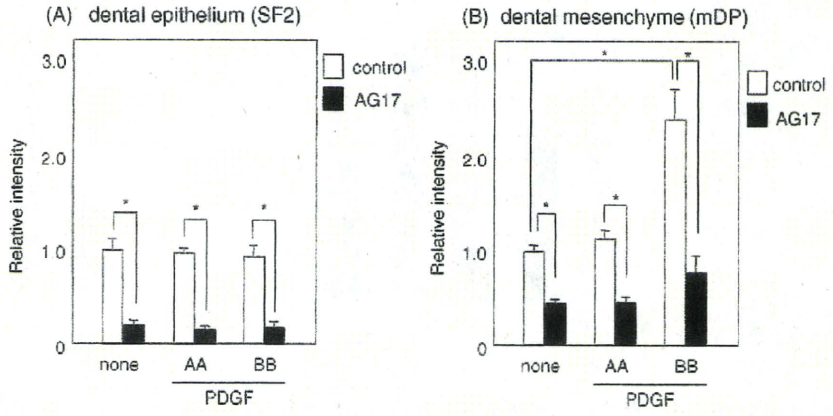

Fig. 4 – AG17 inhibits cell proliferation. The numbers of (A) SF2 cells and (B) mDP cells cultured with or without AG17 were determined using a cell counting kit after 5 days of culture. AG17 inhibited cell proliferation of both SF2 and mDP cells. Neither PDGF-AA nor -BB had effects on SF2 proliferation. However, PDGF-BB promoted mDP cell proliferation, whereas PDGF-AA did not. Statistical analysis was performed using analysis of variance (*, $p < 0.01$).